Bollettino della Società Paleontologica Italiana, 64 (3), 2025, 517-543. Modena

Unusual mass-occurrence of small, uncoiled ammonites in a Barremian black shale of the Maiolica Formation in the Umbria-Marche Basin (Central Italy)

Christian Conti*, Paolo Faraoni, Alan Maria Mancini, Luca Martire & Alessandra Negri*

C. Conti, Dipartimento di Scienze della Terra, Università di Pisa, via Santa Maria 53, I-56126 Pisa, Italy; Museo Brancaleoni di Piobbico, Associazione Neroniade, via Brancaleoni, I-61046 Piobbico, Italy; chri2001conti@gmail.com, christian.conti@phd.unipi.it **corresponding author*
P. Faraoni, via Sparapani 11c, I-60131 Ancona, Italy; paolo.faraoni@libero.it
A.M. Mancini, Dipartimento di Scienze della Vita e dell'Ambiente, Università Politecnica delle Marche, via Brecce Bianche, I-60131 Ancona, Italy; Dipartimento di Scienze Pure e Applicate, Università degli Studi di Urbino Carlo Bo, via Ca' Le Suore 2/4, I-61029 Urbino, Italy; a.m.mancini@staff.univpm.it, alan.mancini@uniurb.it
L. Martire, Dipartimento di Scienze della Terra, Università degli Studi di Torino, via Valperga Caluso 35, I-10125 Torino, Italy; luca.martire@unito.it
A. Negri, Dipartimento di Scienze della Vita e dell'Ambiente, Università Politecnica delle Marche, via Brecce Bianche, I-60131 Ancona, Italy; a.negri@univpm.it
**corresponding author*

KEY WORDS - Leptoceratoididae, paleoecology, paleobiogeography, Barremian, deoxygenation events, Mt. Cipollara, Umbria-Marche Basin.

ABSTRACT - The unique mass occurrence of tiny heteromorph ammonites found in a single layer in the Mt. Cipollara locality of Cerreto d'Esi (Maiolica Formation, Umbria-Marche Basin, Italy) provides critical insights into the depositional environments of the upper portion of the Cretaceous Maiolica Formation. The mechanisms behind the formation and preservation of this ammonite assemblage within black shales remain poorly understood. To address this knowledge gap, we used biostratigraphy and stable carbon isotopes to analyze the entire section containing the layer rich in ammonites. We then conducted a high-resolution paleoecological analysis on this specific layer. Samples were systematically collected across multiple stratigraphic layers to ensure comprehensive coverage. The focus was on documenting the morphology, abundance, and associated sedimentary structures of the ammonite assemblage. Additionally, sedimentological petrographic examinations were carried out to clarify depositional processes.

Our results reveal a diverse ammonite assemblage dominated by the Leptoceratoididae family of early Barremian age, showing relatively good preservation in a predominantly dysoxic, low-energy environment at the seafloor. Calcareous nannofossil data suggest the presence of a well-stratified water column, with a low salinity lid. The multidisciplinary analyses indicate that these black shales not only served as a repository for ammonite remains but also reflected localized paleoecological conditions characterized by reduced turbulence and increased organic deposition. This unique sedimentary and paleontological context suggests that deposition may have been influenced by regional fluctuations in climatic and oceanographic conditions. Consistent with recent literature on Leptoceratoididae, the presence of both normal coiled (oligotrophic) and heteromorphic (mesotrophic) ammonites in the assemblage suggests that the stratification of water masses favored the coexistence of both types, leading to ecological segregation and explaining the paleontological record.

INTRODUCTION

Calcareous rocks of the Umbria-Marche sedimentary succession are of great interest to ammonite paleontologists, especially in Jurassic deposits where well-preserved ammonite remains are abundant. In Cretaceous deposits, although rare and often poorly preserved, these ammonites still hold significance (e.g., Centamore et al., 1971; Cecca & Landra, 1994; Cecca et al., 1995; Faraoni et al., 1998). The rare ammonites are typically found in the Lower Cretaceous sedimentary rocks of the Maiolica Formation (upper Tithonian-lower Aptian), a facies widely distributed in the Western Tethys area (Wieczorek, 1988). They are notably absent from other formations of this sedimentary succession, such as the Marne a Fucoidi Formation, Scaglia Bianca Formation, and Scaglia Rossa Formation. Few ammonite records were reported in the Umbria-Marche Maiolica Fm. before the 1990s (Canavari, 1878; Ramaccioni, 1939; Barbera, 1967; Cecca, 1985). Following the identification of the Faraoni key-bed (Cecca et al., 1994), a comprehensive biostratigraphic study was initiated, leading to a comprehensive Maiolica ammonite-based biozonation (e.g., Cecca et al., 1995; Cecca & Pallini, 1996; Faraoni et al., 1998).

The distribution of ammonites in the water column was influenced by various environmental factors. Near the shelves, their abundance and distribution depended on water depth, currents direction and intensity, sea level, terrigenous input from land, and primary productivity (Cecca, 1998a). In distal epi-oceanic areas (sensu Olòriz, 1990) like the Umbria-Marche Basin (UMB) during the Mesozoic Era, the distribution of ammonite fauna was governed by fluctuations in trophic resources, which were tied to oceanic primary productivity influenced by climatic variability (Cecca, 1998a). Climatic changes played a vital role in determining chemical-physical oceanographic variations. These changes caused stress within communities, leading to modifications in the assemblage and facilitating relatively rapid specific turnover (Westermann, 1990, 1996; Olòriz et al., 1993; Reboulet & Atrops, 1995; Cecca, 1998a, b; Reboulet et al., 2003). Changes observed in some Tethyan basins from the late Hauterivian to early Aptian, characterized by recurring dysoxic conditions, were likely driven

ISSN 0375-7633

doi:10.4435/BSPI.2025.30

by shifts towards warmer and more humid climatic regimes, enhancing nutrient fluxes into oceanic basins and impacting ecosystem ecology (Föllmi et al., 2012). The sedimentary expression of these changes is sometimes represented by organic-rich layers known as black shales.

According to Cecca (1998a), climatic and oceanographic changes during the Barremian period led to a rapid and significant diversification of ammonites by creating new ecological niches and increasing nutrient availability. The Mid-Barremian Event (MBE; Coccioni et al., 2003) is an example of a paleoenvironmental perturbation marked by a positive carbon isotope excursion (+ 0.5‰; Sprovieri et al., 2006). This excursion is seen as evidence of widespread organic carbon deposition, likely due to shifts toward more humid and warmer climatic conditions in the Central Tethys region. The proliferation of certain ammonite families, like Leptoceratoididae Thieuloy, 1966, documented in the Northern Calcareous Alps (Austria; Lukeneder, 2003, 2005) and the Transdanubian Range (Hungary; Gőgös & Szives, 2024), appears to be closely linked to this event.

This paper describes in detail a new outcrop at Mt. Cipollara (Marche region, Italy) where a 27 cm-thick black shale, containing an interesting ammonite assemblage, is found. This black shale shows an unusual number of heteromorph ammonites belonging to Leptoceratoididae, whose ecology and periodic mass occurrences in the paleontological record are poorly documented worldwide and not fully understood. Using an integrated approach (sedimentology, isotope geochemistry, paleontology and paleoecology) we characterized this new black shale aiming to elucidate the environmental mechanisms behind its deposition, and to explore the potential role of Leptoceratoididae as paleoecological indicators, also revising their paleogeographic distribution.

STUDY AREA

Our study is based on material from Mt. Cipollara, Italy (Fig. 1), which, during the Mesozoic Era, was part of the peri-Mediterranean system of the Alpine chain (Menichetti, 2016). The stratigraphic evolution of this area is well-documented in the literature (Colacicchi et al., 1970; Centamore et al., 1971; Farinacci et al., 1981; Galluzzo & Santantonio, 2002; Pierantoni et al., 2013; Fabbi, 2015; Cipriani, 2016). The Umbria-Marche sedimentary succession underwent four stages, beginning in the Jurassic period. The broad and thick Jurassic pelagic platform system, represented by the Calcare Massiccio Fm. (Zittel, 1870; Verri, 1883), was disrupted by the extensional tectonic activity that characterized the Apennine region during the Early Jurassic, leading to uplift and subsidence with varying depositional patterns (Bernoulli, 1967; Colacicchi et al., 1970; Centamore et al., 1971; Farinacci et al., 1981; Bertotti et al., 1993; Santantonio & Carminati, 2011; Fabbi & Santantonio, 2012). In the uplifted areas (structural highs), a condensed succession formed, known as the Bugarone Group ("condensed series" according to Centamore et al., 1971; "facies association A" according to Santantonio, 1993). In the subsiding areas (structural lows), a complete succession was deposited, consisting of the Corniola, Rosso Ammonitico, Calcari a Posidonia, Calcari Diasprigni, and Calcari a Saccocoma e Aptici formations ("complete series" according to Centamore et al., 1971; "facies association B" according to Santantonio, 1993). By the end of the Jurassic period, in the late Tithonian and during the Early Cretaceous, the deposition of the Maiolica Fm. homogenized the lithofacies while maintaining differences in bathymetry between the former structural highs and lows (Menichetti, 2016).

The Maiolica Fm. is characterized by whitish, brownish, or gray micritic limestones, with numerous intercalations of dark marls and very fine siliciclastic layers rich in organic matter (OM), as well as varicolored cherts in bands or nodules. Monotonous sedimentation continued through the deposition of the Marne a Fucoidi Fm. in the early Aptian, evolving towards hemipelagic lithotypes characterized by cherty carbonates and marls during the Late Cretaceous and Paleogene (Menichetti, 2016).

According to the paleomap by Turco et al. (2007), the deposition of the Umbria-Marche Maiolica and Marne a Fucoidi formations occurred in the deep basin formed between the Lazio-Abruzzo carbonate platforms to the southwest and the Adriatic-Dinaric one to the east. The complex physiography inherited from the Jurassic period persisted until the Barremian-Aptian Stages, influencing the thickness of the Maiolica Fm. successions and causing redeposition events (Fabbi, 2015; Menichetti, 2016). Debris flow and slump deposits are frequently observed in the sedimentary record near the structural highs and/or Jurassic faults, which were reactivated during the middle Barremian (Cipriani & Bottini, 2019), across the Barremian-Aptian boundary (Fabbi et al., 2016), and during the Late Cretaceous (Alvarez & Lowrie, 1984). Conversely, far from structural paleo-highs, the sedimentary successions appear predominantly undisturbed.

A gradual increase in black shales is recorded in the upper Maiolica Fm. (upper Hauterivian-lower Aptian), in successions deposited over former paleo-highs or paleo-lows, marking the transition to the overlying Marne a Fucoidi Fm. The deposition of the latter occurred in a homogeneous paleobathymetric context, as indicated by its regular thickness. Pelagic carbonate-dominated sedimentation in UMB continued in the Upper Cretaceous-Paleogene with the deposition of the Scaglia Group (Scaglia Bianca, Scaglia Rossa, Scaglia Variegata, and Scaglia Cinerea formations). Subsequently, starting from the Miocene, increased clay input led to the deposition of marly limestones and calcareous marls of the Bisciaro Fm. and Schlier Fm. This last is heteropic with the foredeep deposits of the Marnoso Arenacea Fm.

→

Fig. 1 - (color online) Geographical and geological setting of the Mt. Cipollara section. a-b) Section location (red star). Scale bars correspond to 250 km (a) and 2 km (b). c) Geological setting of the Mt. Cipollara locality (scale 1:10.000). The black line remarks the road (SP14) between Cerreto d'Esi and Poggio San Romualdo localities, also visible in (b). The red line indicates the studied Mt. Cipollara outcrop.

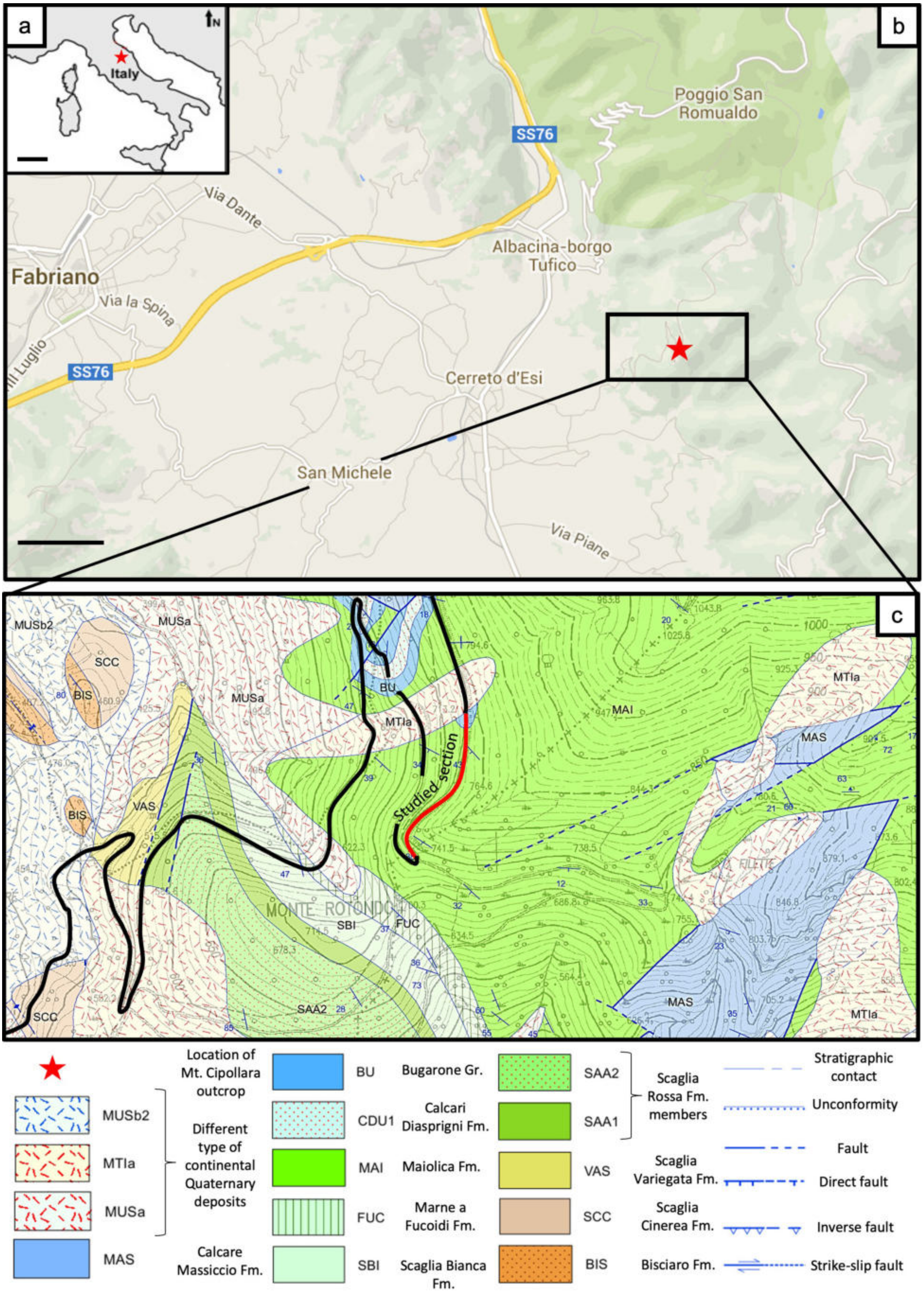
a
N
Italy
b
Poggio San Romualdo
SS76
Via Dante
Albacina-borgo Tufico
Fabriano
Via la Spina
Cerreto d'Esi
San Michele
Via Piane
c
MUSb2
MUSa
SCC
BIS
BU
MTIa
MAI
MAS
VAS
Studied section
MONTE ROTONDO
SBI
FUC
SAA2
Location of Mt. Cipollara outcrop
MUSb2
MTIa
MUSa
Different type of continental Quaternary deposits
MAS
Calcare Massiccio Fm.
BU
Bugarone Gr.
CDU1
Calcari Diasprigni Fm.
MAI
Maiolica Fm.
FUC
Marne a Fucoidi Fm.
SBI
Scaglia Bianca Fm.
SAA2
SAA1
Scaglia Rossa Fm. members
VAS
Scaglia Variegata Fm.
SCC
Scaglia Cinerea Fm.
BIS
Bisciaro Fm.
Stratigraphic contact
Unconformity
Fault
Direct fault
Inverse fault
Strike-slip fault

MATERIAL AND METHODS

The Mt. Cipollara section

The Mt. Cipollara section (43°19’36”N 13°01’26”E) is in the central part of the Marche ridge, extending in the NNW to SSE direction between the Esino and Potenza rivers. The succession, outcropping along the provincial street (SP14, km 5) between Cerreto d’Esi and Poggio San Romualdo (Fig. 1b), encompasses the upper Bugarone Fm. and a large interval of the Maiolica Fm., with a total thickness of 230 meters. The section starts where the first Bugarone bed (15 cm-thick) is observed, onlapping the Calcari Diasprigni Fm. The Bugarone Fm.-Maiolica Fm. boundary is detected 20 m above the base of the section. At Mt. Cipollara, the Maiolica Fm., even if poorly exposed due to debris and vegetation cover, appears as fine decimetric, white-ivory limestone layers alternating with cherty layers, locally occurring in bands or nodules. In the upper part of the section, the lithology gradually changes upward, showing increasing marly limestones with a grayish color, locally laminated and alternated with black shales, millimeter to centimeter thick. In the upper 35 m of the studied section at least 16 beds identifiable as black shale are observed. Finally, in the last 9 meters of the section, four beds of matrix-supported intraclastic floatstones referable to debris flow phenomena are detected, ranging in thickness from 22 to 50 cm (Fig. 2b).

The focus of this work is a 27 cm-thick bed of black shales in the upper Maiolica Fm. that we found to be rich in small ammonites (Mt. Cipollara Level, MCL; Figs 2a, 3). The MCL’s thickness fluctuates slightly throughout the outcrop, due to dissolution and/or wavy contact with the

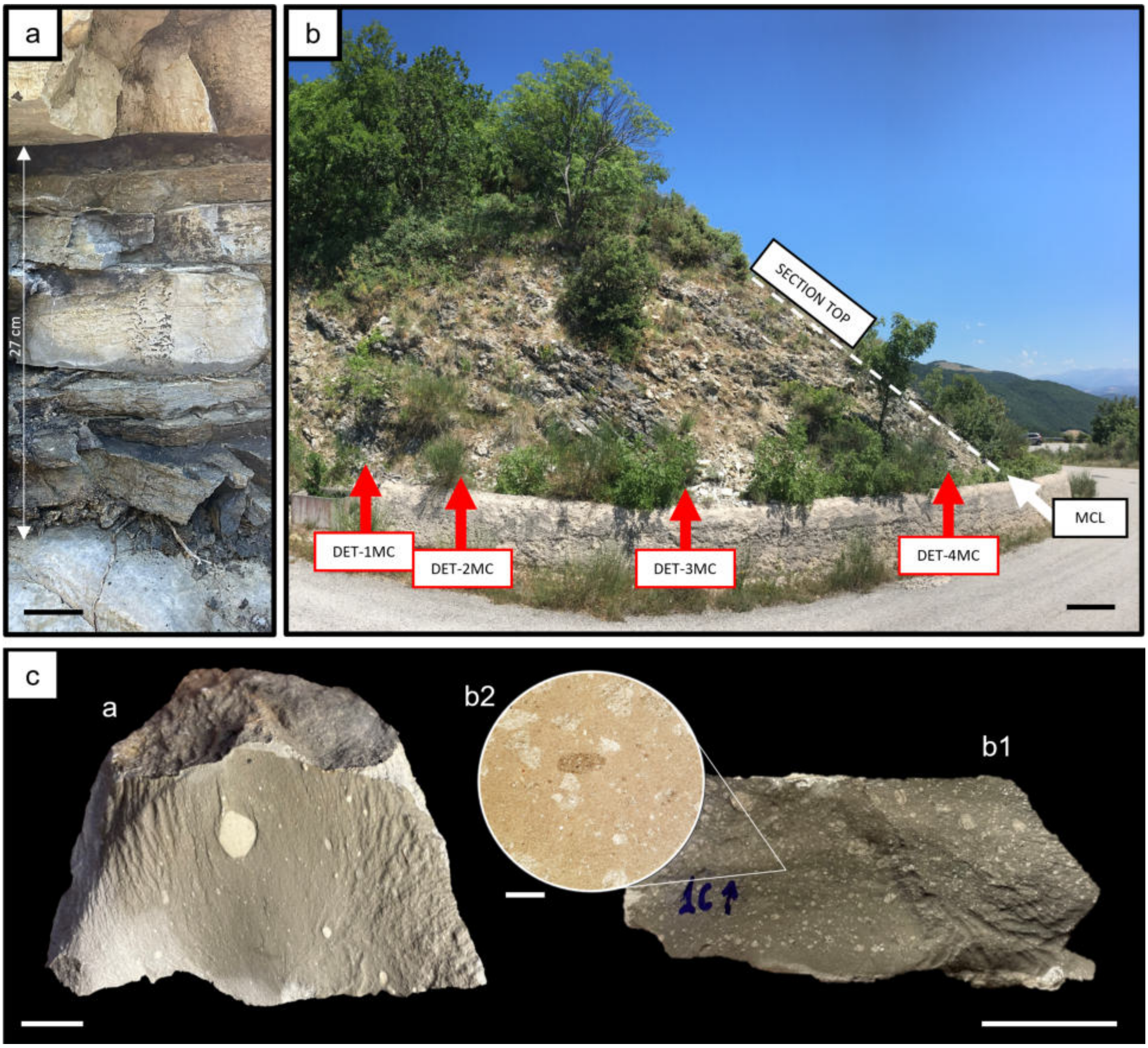

Fig. 2 - (color online) Details on the last portion of the Mt. Cipollara section. a) Outcrop view of the MCL. Scale bar corresponds to 5 cm. b) Stratigraphic position of matrix-supported intraclastic floatstones layers (red boxes) and of the MCL. Scale bar corresponds to 1 m. c) Mesoscale and microscale lithological characters of two representative samples of matrix-supported intraclastic floatstones of the layers DET-3MC and DET-4MC. Scale bars for (a) and (b1) correspond to 1 cm; scale bar for (b2) corresponds to 500 µm.

top limestone. Three intervals (Fig. 3) can be distinguished within the MCL, which are described from the bottom to the top as follows:

1. Lower interval: a 10 cm-thick interval, consisting of 1 cm of finely laminated marlstone followed by 3 cm of finely laminated calcareous mudstone. Above, a centimetric mudstone layer containing millimetric to sub-millimetric muddy clasts, slightly lighter in color than the surrounding matrix is observed. The contact between the laminated mudstones and the mud-supported clastic layer is wavy. Variation in thickness of the mudstone clastic layer is observed. The maximum thickness recorded is 7 cm. This clastic level onlaps on calcareous laminated mudstone, ranging from 1 to 5 cm. The upper portion of the laminated mudstone grades into 1 cm of very finely laminated marlstone, corresponding to sample F1bis. The mass occurrence of ammonites is within the laminated calcareous mudstones of the lower interval of the MCL.
2. Middle interval: a 7 cm-thick interval, characterized by a 5 cm-thick massive grey mudstone layer, overlain by 2 cm of faintly laminated mudstone. Very small, scattered muddy clasts, slightly lighter in color than the surrounding matrix, are observed. Ammonites are present in this interval, although they are less abundant than in the lower interval.
3. Upper interval: ten to 13 cm-thick, the interval is characterized by 9 cm of calcareous laminated mudstones overlain by 2 cm of dark claystone. Two cm above the base of the interval, a 2 mm-thick dark clay interlayer is observed. In this interval, wavy lamination substitutes plane parallel lamination in some places. The upper portion is represented by dark, calcareous, very fine laminated marlstones, 2 to 4 cm thick, replaced in some places by white calcareous lenses.

Samples at the base and top of the MCL are named MCSC12A and MCSC12B, respectively (Fig. 3).

Stable isotopes

Stable carbon isotope ($\delta^{13}C$) analyses were conducted on the Maiolica Fm. at low resolution sampling (one sample every 20 m, starting from sample 2; Fig. 3). The analyses were performed using an automated carbonate preparation device (Gasbench II) and a Thermo Fisher Scientific Delta V Advantage continuous flow mass spectrometer at the Dipartimento di Scienze della Terra, Università degli Studi di Milano. Carbonate powder samples were reacted with > 99% orthophosphoric acid at 70 °C. The stable carbon isotope compositions are expressed in the conventional delta notation calibrated to the Vienna Pee-Dee Belemnite (V-PDB) scale by international standards IAEA 603 and NBS-18. Analytical reproducibility for these analyses was better than ± 0.1‰.

Calcareous nannofossils

The study was conducted using simple smear slides (Bown & Young, 1998), analyzed with a light polarizing ZEISS microscope, at 1250x magnification. The representative taxa of the calcareous nannofossils (CN) assemblages of the MCL are shown in Fig. 4. Samples were prepared as smear slides by putting a small amount of powdered sediment on a cover-glass adding a few drops of distillate water, without centrifuging, ultrasonic cleaning, or settling the sediment, thus retaining the original rock composition.

Biostratigraphic qualitative analyses of the whole section were performed at low-resolution sampling (one sample every 20 meters; Fig. 3). The biostratigraphic framework is based on CN Zones after Sissingh (1977), with modification by Perch-Nielsen (1979, 1985) and Applegate & Bergen (1988). Correlations of biostratigraphic data were also made according to Erba & Quadrio (1987).

High-resolution sampling (20 samples in 27 cm; Fig. 3) has been carried out to detail the CN assemblages characterizing the MCL.

For classification we follow Perch-Nielsen (1985). Some genera and species are updated to the classification of Bown et al. (1998) also through the website mikrotax (Young et al., 2022).

Taxa were identified at species level, then grouped at generic level as in Tremolada et al. (2009), with some specified modifications. Both wide-canal and narrow-canal nannoconids were incorporated into the total count of nannoconids. The narrow-canal group mainly consists of *Nannoconus steinmannii* Kamptner, 1931, with low abundances of *N. bermudezii* Brönnimann, 1955, and *N. colomii* De Lapparent, 1931, whereas wide-canal forms are represented by *N. bucheri* Brönnimann, 1955, *N. kamptneri* Brönnimann, 1955, *N. circularis* Deres & Achéritéguy, 1980 and *N. globulus* Brönnimann, 1955. Other groupings include *Watznaueria* spp. Reinhardt, 1964 (*W. barnesiae* Black in Black & Barnes, 1959 and minor percentages of *W. ovata* Bukry, 1969, *W. fossacincta* Black, 1971a, *W. supracretacea* Reinhardt, 1965, and *W. britannica* Stradner, 1963 and pentaliths (*Micrantholitus obtusus* Stradner, 1963, *Micrantholitus hoschulzii* Reinhardt, 1966, and *Braarudosphaera regularis* Black, 1973). *Assipetra terebrodentarius* Applegate, Bralower, Covington & Wise in Covington & Wise, 1987 was grouped to generic level with *Assipetra infracretacea* Thierstein, 1973. Species displaying low abundances such as *Zeugrhabdothus embergeri* Noël, 1959, *Z. diplogrammus* Deflandre in Deflandre & Fert, 1954, *Z. erectus* Deflandre in Deflandre & Fert, 1954, *Rhagodiscus asper* Stradner, 1963, *R. splendens* Deflandre, 1953, *Retecapsa angustiforata* Black, 1971b, *Diazomatholithus lehmanii* Noël, 1965, *Lithraphidites carniolensis* Deflandre, 1963, *Staurolithus stradneri* Rood, Hay & Barnard, 1971 and *Cyclagelosphaera margerelii* Noël, 1965 were grouped in "other species."

The preservation was evaluated as follows: 1) good-little or no evidence of dissolution and/or secondary recrystallization, diagnostic characters completely preserved; 2) moderate-secondary dissolution and/or recrystallization, primary morphological characters partially altered, almost all specimens can be determined to a specific level; 3) poor-strong dissolution, fragmentation, and/or secondary recrystallization, altered primary morphological characters, many specimens cannot be determined at the specific and/or genus level.

Quantitative analyses were conducted on the 20 samples from the MCL (Fig. 3). In smear slides, nannofossil assemblages were quantified by counting at least 300 specimens and then percentages of a single taxon with respect to the total nannoflora (relative abundance)

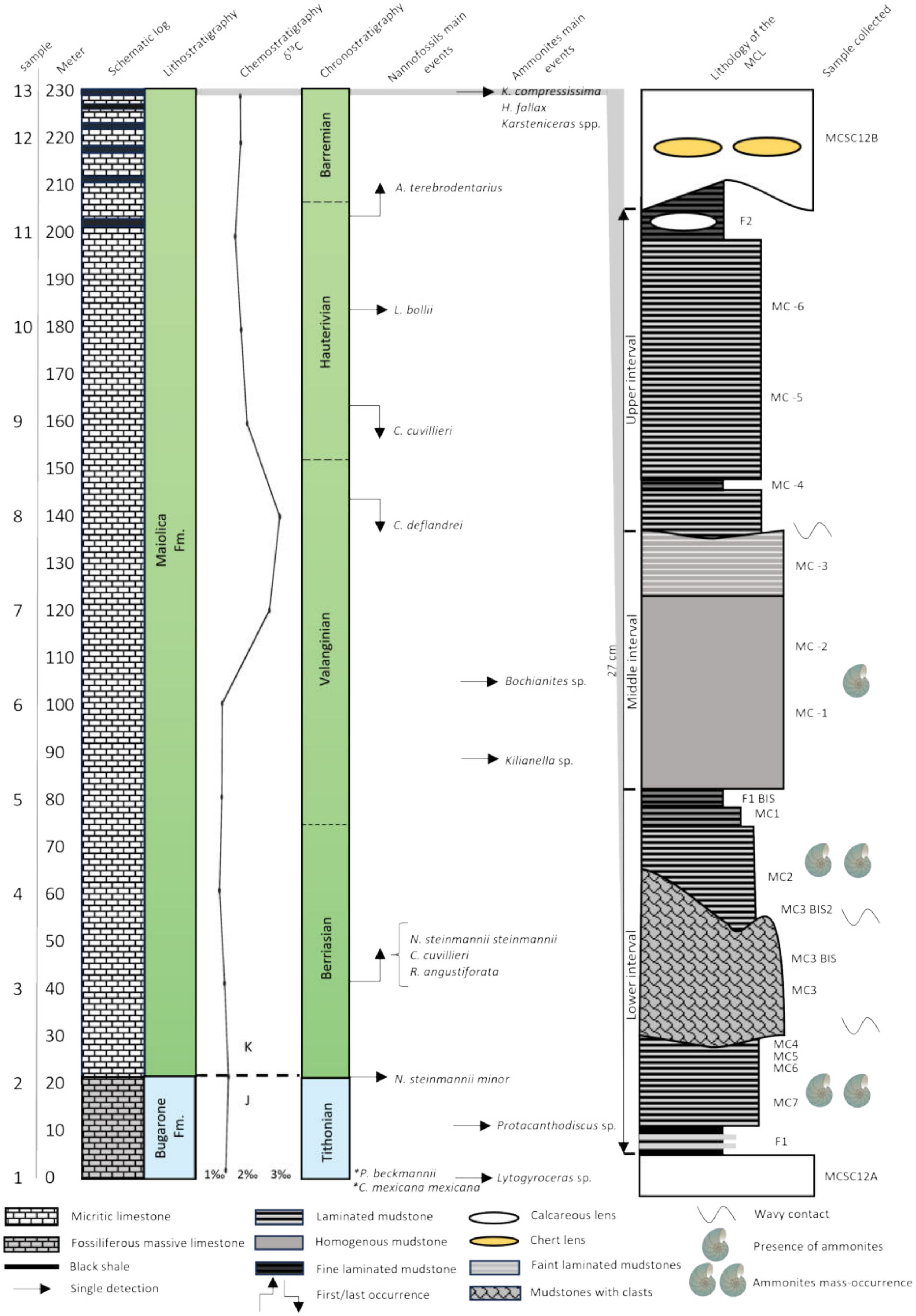
sample
Meter
Schematic log
Lithostratigraphy
Chemostratigraphy δ13C
Chronostratigraphy
Nannofossils main events
Ammonites main events
Lithology of the MCL
Sample collected
13 230
12 220
210
11 200
190
10 180
170
9 160
150
8 140
130
7 120
110
6 100
90
5 80
70
4 60
50
3 40
30
2 20
10
1 0
Maiolica Fm.
Bugarone Fm.
1‰ 2‰ 3‰
K
J
Barremian
Hauterivian
Valanginian
Berriasian
Tithonian
A. terebrodentarius
L. bollii
C. cuvillieri
C. deflandrei
N. steinmannii steinmannii
C. cuvillieri
R. angustiforata
N. steinmannii minor
*P. beckmannii
*C. mexicana mexicana
K. compressissima
H. fallax
Karsteniceras spp.
Bochianites sp.
Kilianella sp.
Protacanthodiscus sp.
Lytogyroceras sp.
Upper interval
Middle interval
Lower interval
27 cm
MCSC12B
F2
MC -6
MC -5
MC -4
MC -3
MC -2
MC -1
F1 BIS
MC1
MC2
MC3 BIS2
MC3 BIS
MC3
MC4
MC5
MC6
MC7
F1
MCSC12A
Micritic limestone
Fossiliferous massive limestone
Black shale
Single detection
Laminated mudstone
Homogenous mudstone
Fine laminated mudstone
First/last occurrence
Calcareous lens
Chert lens
Faint laminated mudstones
Mudstones with clasts
Wavy contact
Presence of ammonites
Ammonites mass-occurrence

were calculated. The total abundance was calculated by counting specimens per field of view (FOV) on smear slide areas as homogeneous as possible and was expressed as follows: Common (C): ten-20 specimens per FOV; Frequent (F): five-nine specimens per FOV; Rare (R): one-four specimens per FOV.

We considered that nannoconids can be underestimated in smear slides, essentially owing to mechanical breakage during powdering. In fact, their ultrastructure favors the disintegration of single crystals (Noël & Melguen, 1978). Smear slides and raw samples are deposited at the Dipartimento di Scienze della Vita e dell'Ambiente, Università Politecnica delle Marche, Laboratorio di Stratigrafia, Sedimentologia e Paleoecologia (Paleolab).

Ammonites

Taxonomic analyses were conducted on 182 ammonite samples of which 21 collected over the entire Mt. Cipollara section and 161 collected from the MCL (see Supplementary Online Material [SOM]). The most complete, well-preserved, and representative specimens of the MCL assemblage are shown in Pls 1 and 2. The specimens are shown in black and white without having been coated with ammonium chloride. Identification of ammonites was made following Wright et al. (1996) and Klein et al. (2007). The distinction between *Karsteniceras* Royo Y Gomez, 1945 and *Leptoceratoides* Thieuloy, 1966 was made following Gőgös & Szives (2024). We used the latest Tethyan (Standard Mediterranean Ammonite Zonation) stratigraphic scheme recently updated by Szives et al. (2023).

The preparation of samples took place through simple washing or liberation from the sediment where necessary using pneumatic tools. All the material is deposited at Museo Civico Brancaleoni of Piobbico, Neroniade Geopaleontological Observatory.

Sedimentary petrography of MC

Four samples (MC3 BIS2, MC2, MC -2 and MC -5; Fig. 3) were prepared by carrying out an epoxy impregnation and cutting a slice perpendicular to the bedding; two sediment stubs from the freshly broken sample MC2 (the ammonite-richest) were carbon-coated for investigation with JMS-IT300LV Scanning Electron Microscope (SEM). Semi-quantitative characterization of the main elements was performed during SEM investigation using energy-dispersive spectroscopy (EDS) Oxford Instrument Link System microprobe. The samples were also analyzed with an optical microscope at different magnification with transmitted and reflected light.

RESULTS

Stable isotopes

Figure 3 reports the $\delta^{13}C$ curve of the Mt. Cipollara section. It shows, from sample 1 to sample 6, values around 1.5‰ with minimal fluctuations. Subsequently, a positive shift increases the $\delta^{13}C$ to 3‰ between sample 7 and 8. From sample 9, values decrease and are around 2‰, remaining stable up to the top of the section.

Calcareous nannofossils

LOW RESOLUTION ANALYSIS OF MT. CIPOLLARA SECTION - Calcareous nannofossils (CNs) are present in all the analyzed samples, although they are generally poorly preserved. Several markers have been found in the samples (Fig. 3) collected from the base to the top of the section: specifically, *Conusphaera mexicana mexicana* Trejo, 1969 and *Polycostella beckmannii* Thierstein, 1971 are observed at the base of the section (sample 1); *N. steinmannii minor* Deres & Achéritéguy, 1980 was only found in sample 2; *N. steinmannii steinmannii* and *R. angustiforata* are present from sample 3 to the top of the section. *Cruciellipsis cuvillieri* Manivit, 1966 ranges from sample 3 to sample 9; *Cyclageloshaera deflandrei* Manivit, 1966 is present from sample 1 to sample 8; *Lithraphidites bollii* Thierstein, 1971 is observed only in sample 11. Finally, *A. terebrodentarius* occurs from sample 11 up to the top of the section.

CALCAREOUS NANNOFOSSIL ASSEMBLAGE CHARACTERIZING THE MCL - Relative CN abundances are shown in Fig. 5. The study of samples taken from the two layers immediately below and above the MCL (samples MCSC12A and MCSC12B; Fig. 3) shows the common characteristics of the Maiolica Fm., with samples affected by intense recrystallization and almost entirely consisting of micarbs. CNs are rare in these samples (with an average of one specimen per FOV). The assemblages appear dominated by highly calcified species such as nannoconids and *Watznaueria*. Nannoconids show values between 25 and 30% while *Watznaueria* spp. (with the major contribution, almost exclusive, of *W. barnesiae*) shows values between 44 and 50%. Moreover, in samples MCSC12A and MCSC12B, *Watznaueria* spp. is slightly more abundant than nannoconids. Pentaliths are rare, reaching just 2% in MCSC12A, while the *Assipetra* group is common with values around 10%. Among the other species, representing 12% of the assemblage, *Z. embergeri*, *R. angustiforata*, *R. asper* and *L. carniolensis* stand out.

Quantitative analysis of homogeneous areas in smear slides highlights a frequent to common occurrence of specimens within the MCL, with an average of seven specimens per FOV. In contrast, they are rare in the bioturbated Maiolica Fm. of samples MCSC12A and MCSC12B. The greatest abundance of CNs within the MCL compared to the bioturbated Maiolica Fm. cannot be due to better preservation within the MCL, since even resistant and highly calcified forms such as nannoconids and *Watznaueria* spp. are less abundant in samples MCSC12A and MCSC12B (abundance column in Fig. 5). The analysis evidences a generally moderate preservation with slight dissolution in marlstone layers, especially in

◄

Fig. 3 - (color online) Lithostratigraphy, chronostratigraphy, chemostratigraphy and the main biostratigraphic calcareous nannofossil and ammonite events recorded in the section studied. The asterisk in the "main calcareous nannofossils event" column indicates that a taxon occurs since the base of the section. On the right, the closeup log describes in detail the black shale level containing abundant ammonites.

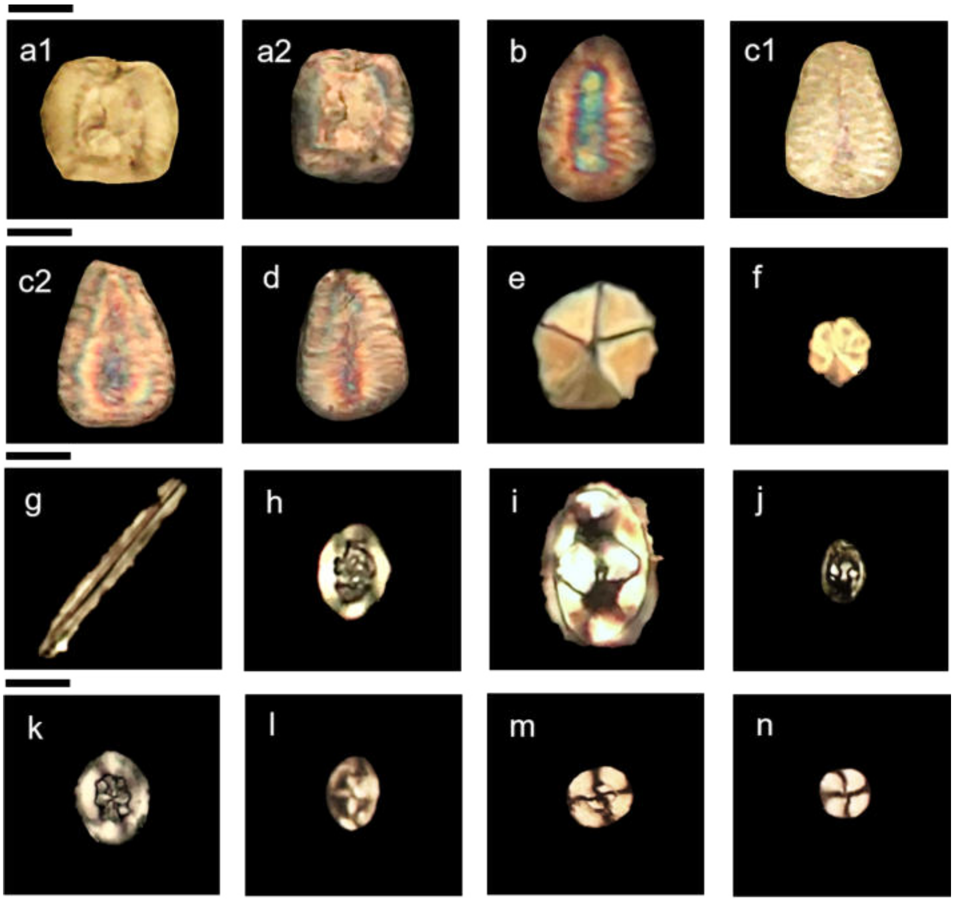

Fig. 4 - (color online) Most common calcareous nannofossil species found in the MCL. a1) *Nannoconus globulus* Brönnimann, 1955, Mt. Cipollara section. Sample F1. PPL. a2) Same specimen, Mt. Cipollara section. Sample F1. XPL. b) *Nannoconus kamptneri* Brönnimann, 1955, Mt. Cipollara section. Sample F2. XPL. c1) *Nannoconus colomii* De Lapparent, 1931, Mt. Cipollara section. Sample F2. PPL. c2) Same specimen, Mt. Cipollara section. Sample F2. XPL. d) *Nannoconus steinmannii* Kamptner, 1931, Mt. Cipollara section. Sample F1. XPL. e) *Micrantholithus hoschulzii* Reinhardt, 1966, Mt. Cipollara section. Sample MC2. XPL. f) *Assipetra terebrodentarius* Applegate, Bralower, Covington & Wise, 1987, Mt. Cipollara section. Sample F1bis. XPL. g) *Lithraphidites carniolensis* Deflandre, 1953, Mt. Cipollara section. Sample MC1. XPL. h) *Rhagodiscus asper* Stradner, 1963, Mt. Cipollara section. Sample MC2. XPL. i) *Zeugrhabdothus embergeri* Noël, 1959, Mt. Cipollara section. Sample F2. XPL. j) *Zeugrhabdothus erectus* Deflandre, 1954, Mt. Cipollara section. Sample F1bis. XPL. k) *Retecapsa angustiforata* Black, 1971b, Mt. Cipollara section. Sample F2. XPL. l) *Staurolithus stradneri* Rood, Hay & Barnard, 1971, Mt. Cipollara section. Sample F2. XPL. m) *Watznaueria barnesiae* Black, 1959, Mt. Cipollara section. Sample F2. XPL. n) *Cyclagelosphaera margerelii* Noël, 1965, Mt. Cipollara section. Sample F2. XPL. XPL = cross-polarised light. PPL = plane-polarised light. Scale bars: 5 µm.

sample F1bis. Micarbs (Cook & Egbert, 1979; Beltran et al., 2009) dominate in mudstone layers (both laminated and homogeneous). Independent of lithology, fragile and delicate taxa such as *Biscutum constans* Górka, 1957, *Zeughrabdothus erectus*, and *Discorhabdus ignotus* Górka, 1957 are rare or absent. In the MCL, nannoconids and *Watznaueria* spp. dominate the assemblage in all the samples studied. Nannoconids show a percentage between 27 and 61%. The highest abundance of nannoconids is recorded within mudstones whereas they are less abundant in finely laminated marlstones, with values ranging between 27 and 38%. *Watznaueria* spp. shows frequencies ranging from 17 to 48% of the assemblage with the greatest abundance found in the millimetric laminated marlstone intercalations F1bis and MC -4. In the two black shales F1 and F2, *Watznaueria* spp. shows values compared to those found within mudstones (20-30%). Pentaliths (and their fragments) occur in all the samples studied, with the highest values (6 to 16%) in laminated mudstones. Here very large specimens (14 microns in height) are observed. The lowest values of pentaliths are recorded within the F1bis, MC -4 and F2 marlstone interlayers while they are more abundant in F1. The *Assipetra* group occurs through the interval analyzed with abundance varying from 4 to 17%. Its abundance seems trendless. However, worth noting is the fact that the highest value observed corresponds to the nannoconids negative peak (sample F1bis). Other species vary from 1 to 17%. The major contribution is made by *Z. embergeri*, *R. angustiforata*, *R. asper* and *L. carniolensis*. Large specimens of *Z. embergeri* (14 microns) are common throughout the interval.

Ammonites

Ammonites are rare in the section while they are abundant in the MCL. Figure 3 shows the main ammonite events recorded in the Mt. Cipollara section. Well preserved specimens belonging to *Lytoceras* Suess, 1865

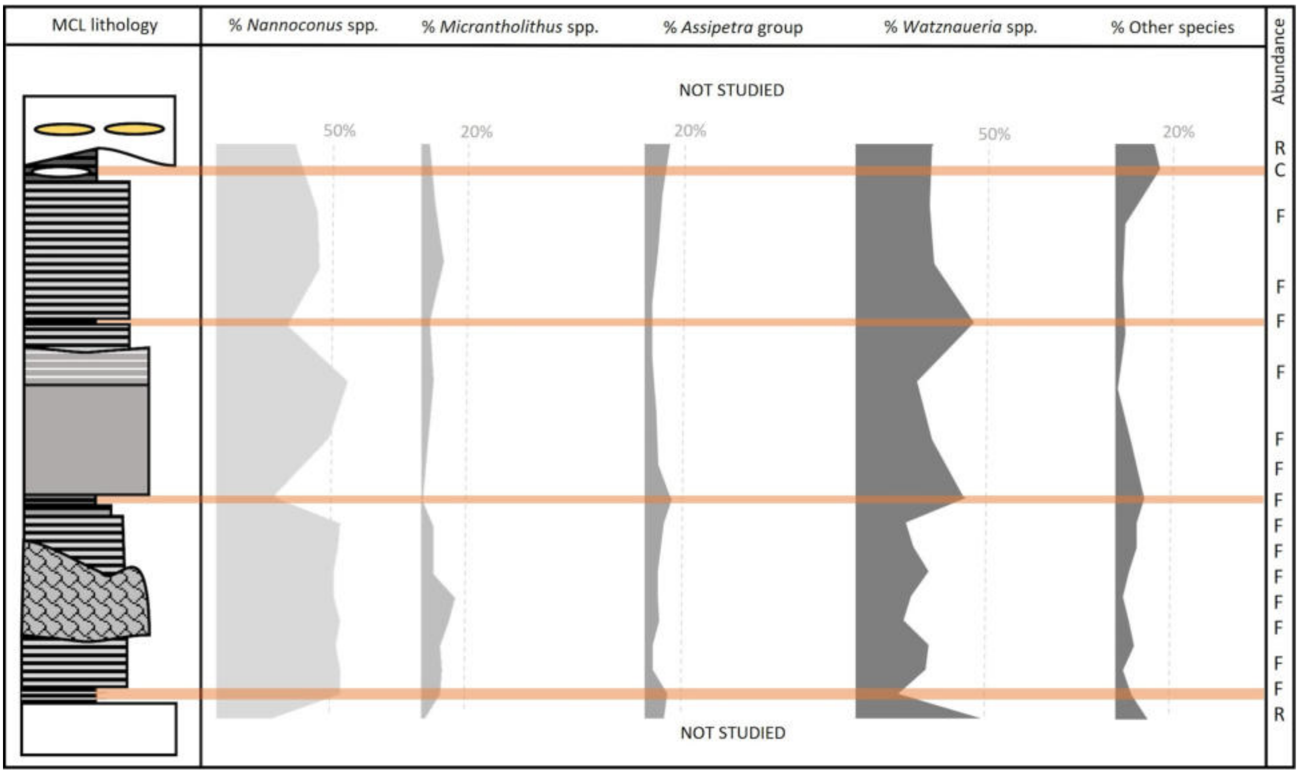

Fig. 5 - (color online) Results of the smear-slide quantitative investigations across the MCL. See Fig. 3 for the lithological description. The "Abundance" column on the right shows the total abundance of calcareous nannofossils in the analyzed samples: C = Common; F = Frequent; R = Rare.

and *Lytogyroceras* Spath, 1925 were found one meter above the base of the section. Other specimens belonging to *Phylloceras* Suess, 1865, *Calliphylloceras* Spath, 1927, *Protacanthodiscus* Spath, 1923, *Virgatosphinctes* Uhlig, 1910 and *Aulacosphinctes* Uhlig, 1910, are collected from meter 12 of the section. At meter 82, two poorly preserved specimens belonging to *Kilianella* Uhlig, 1905 were recorded. From meter 100 a badly preserved specimen of the genus *Bochianites* Lory, 1898 is reported. Upward, at meter 200, two faintly preserved specimens belonging to *Kotetishvilia* Vermeulen, 1996 are found.

As for the MCL, ammonites are small and moderately preserved. They mainly occur within laminated mudstones of the lower interval, especially in correspondence with the sample MC2, while some specimens are detected within the more massive middle interval (Fig. 3). Specimens are preserved as internal molds, showing thin dark organic films, interpreted as remnants of the periostracum, dotted by framboidal pyrite crystals. They are also flattened by sediment compaction. The ventral area was not observed in the specimens collected. Either complete specimens or fragments have been found, all showing a single side only. Juvenile growth stages are visible only on some specimens while the suture line is visible exclusively in one specimen (Cod. MC020BS; Pl. 2, fig. 14). The typical Mediterranean assemblage is dominated by Leptoceratoididae (36%) represented in the level by small specimens, between 0.5 and 3 cm in size (80% of specimens are between 1-2 cm in size). This ammonite family includes 12 genera (Klein et al., 2007). Two of these, *Karsteniceras* and *Leptoceratoides* are common and abundant in analogous Leptoceratoididae-rich mudstone levels (Rieber, 1977; Lukeneder, 2003, 2005; Gőgös & Szives, 2024). They show very similar morphological features which over the years have greatly complicated their distinction, also considering the fact that these ammonites are small, subject to sexual dimorphism (e.g., Lukeneder, 2003) and usually found in lithologies (dark clay or clay-shale deposits) that do not allow the observation or preservation of taxonomically important elements (Lukeneder, 2003). Recently, Gőgös & Szives (2024) remarked that the most important generic feature for their distinction is that no ventrolateral tuberculation or spines are present in *Leptoceratoides*, which clearly marks the difference from *Karsteniceras*. Based on the above-described features, the specimens found inside the MCL can be attributed both to *Leptoceratoides* and *Karsteniceras.* The latter is dominant in the Leptoceratoididae assemblage (71% vs 29%; Fig. 6b). Their classification at the species level is often uncertain due to preservation. In Pl. 2, some clearly identifiable specimens are reported, like *L. ternbergense* Lukeneder & Tanabe, 2002 (Pl. 2, figs 1-6), *K. ibericum* Vašíček & Wiedmann, 1994 (Pl. 2, fig. 7) and *K. beyrichoide* Vašíček & Wiedmann, 1994 (Pl. 2, fig. 8). Figures 9-14 in Pl. 2 illustrate some uncertain species, belonging to *Karsteniceras*, on a total of 22 identified as a group of specimens with similar ornamentation characters not attributable to species described so far. Given the absence of studies regarding the Leptoceratoididae in the UMB area we cannot exclude that these morphologies may belong to a new species. Because of the paleoecological relevance of these ammonites, we believe it is important to illustrate these uncertain forms to fully document the association of Leptoceratoididae found within the MCL.

No specimens of *Karsteniceras* or *Leptoceratoides* were found above and below the MCL. The family Holcodiscidae Spath, 1923 is common (12%), with the genus *Holcodiscus* Uhlig, 1882 and *Astieridiscus* Kilian, 1910. We report *Holcodiscus fallax* Spath, 1924, *Holcodiscus* cf. *nodosus* Karakasch, 1907 and *Astieridiscus* cf. *morleti* Kilian, 1889. Desmoceratidae Zittel, 1895 are consistently present in the level (9%), mostly represented by the genus *Barremites* Breskovski, 1977. Pulchelliidae Douvillè, 1890 (6%) are represented with the genus *Kotetishvilia* Vermeulen, 1996. The latter occurs as the marker-species *Kotetishvilia compressissima* d'Orbigny, 1841. Other species found within MCL are: *Lytoceras* sp., *Lytoceras subfimbriatum* d'Orbigny, 1841, *Protetragonites* sp. Hyatt, 1900, *Phylloceras* sp., *Hypophyllocetas paquieri* Sayn, 1920, *Phyllopachiceras infundibulum* d'Orbigny, 1840, *Moutoniceras* sp. d'Orbigny, 1850, *Anahamulina* sp. Hyatt, 1900, *Anahamulina* cf. *lorioli* Uhlig, 1883, and *Hamulina* sp. d'Orbigny, 1850. In general, normal coiling ammonites dominate over heteromophs (64% vs 36%, Fig. 6c). Due to the preservation state and the small size of some specimens, 16% of the collected material is indeterminate (Fig. 6a).

Petrographic and sedimentological analysis of MCL

The samples analyzed are mudstones, typically faintly to finely laminated, except for samples MC3 BIS2 and MC -2 which are partially or completely massive. Sample MC3 BIS2 is characterized by the presence of white lithoclasts that are coarser grained than the matrix (Fig. 7e), while MC -2 is more homogeneous (Fig. 7f). The lamination in the other samples is wavy and parallel to the bedding and locally interrupted by burrows (Fig. 7a). The lamination consists of alternating light (white-grey) and dark (brown-black) laminae, composed of peloids and terrigenous grains, respectively. The terrigenous nature of the minerals is indicated by the presence of K, Al and Si ions in the SEM-EDS investigation (spectra 2-3 in Fig. 8a; spectra 1, 3 in Fig. 8d). The light laminae are thicker (on average 200 μm) than the dark ones. The matrix is micrite, partially made up of nannofossils (Fig. 7h). Abundant circle-shaped microfossils, resembling radiolarians, punctuate the sediment (Fig. 7c2, d). These microfossils are filled with calcite cement. Broken thin shells of unknown origin (Fig. 7c1, d), scattered phosphatic remains (Figs 6g1; spectrum 1 in Fig. 8c) attributable to fish bones, and clay or quartz minerals 5-30 μm in size, are also present (spectra 1-3 in Fig. 8a; spectrum 2 in Fig. 8b; spectrum 2 in Fig. 8c; spectra 1, 3 in Fig. 8d). Pyrite framboids are scattered and associated with the presence of sediment.

DISCUSSION

Biostratigraphy and chronostratigraphy

The section begins with the Tithonian portion of the upper Bugarone Fm. overlaid by the Lower Cretaceous Maiolica Fm. Here the CN assemblage allows us to assign the interval to the CC1-CC6 Zones (Sissingh, 1977) spanning the Berriasian to the Barremian.

Additionally, the $\delta^{13}C$ isotope positive fluctuation, found between 100 and 160 m, is consistent with the carbon perturbation known in the literature as the "Weissert Event" (Erba, 2004). According to these

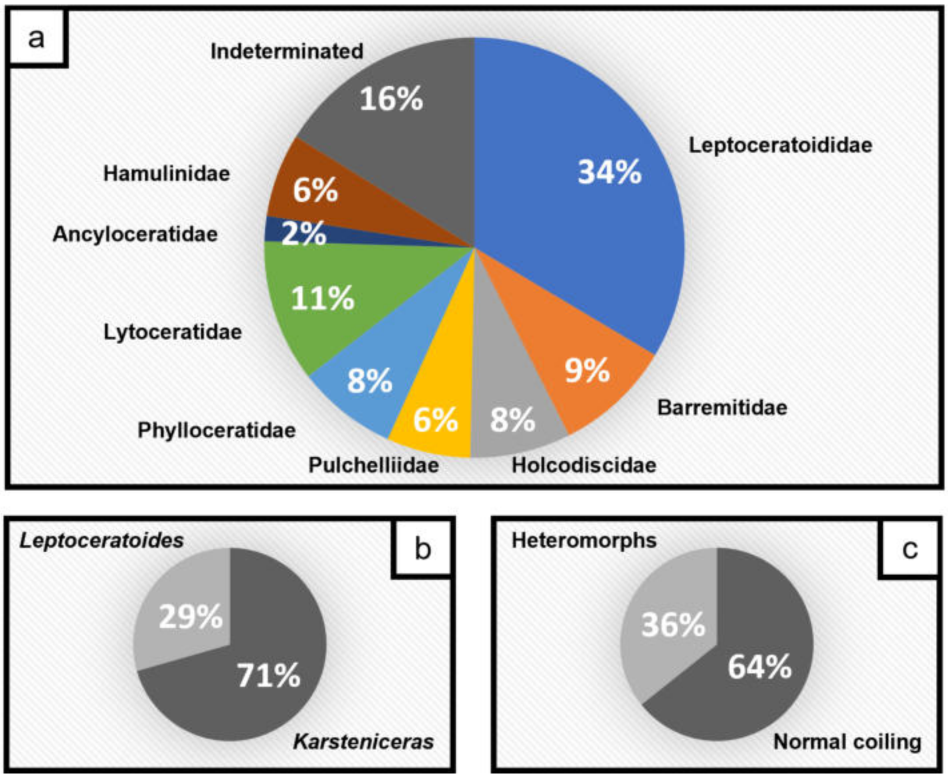

Fig. 6 - (color online) Ammonite assemblage of the MCL. a) Pie chart showing the percentage of ammonite families identified in the MCL. b) Relative abundances of *Leptoceratoides* and *Karsteniceras* within the assemblage. c) Ratio of heteromorphic versus normally coiled ammonites.

authors, the δ^{13}C positive shift is observed from the upper CC3b to the upper CC4a CN subzones (upper Valanginian to early Hauterivian). This, along with the first occurrence of the marker *L. bollii* observed in sample 11, suggests at least a Hauterivian age for the base of the MCL. The base of the MCL is 60 m above the carbon isotope peak of the Weissert Event and 28 m above the unique sample recording the occurrence of *L. bolli.* The presence of *Kotetishvilia compressissima* and *Holcodiscus fallax* further refines the age of the MCL. Based on the most recent standard Mediterranean ammonite zonation (Szives et al., 2023), *K. compressissima* marks the base of the homonymous Zone of the lower Barremian Stage. This Zone is further divided into two subzones (Reboulet et al., 2017; Szives et al., 2023) with the lower characterized by the presence of *Holcodiscus fallax.* Therefore, the MCL falls within the *K. compressissima* Zone, *H. fallax* subzone of the lower Barremian. The *K. compressissima* Zone correlates to the CC6 CN Zone of Sissingh (1977). According to the detailed chronology of Martinez et al. (2020), the base of the *K. compressissima* Zone is dated at 124.97 ± 0.12 Ma for a duration of 0.31 My while the *H. fallax s*ubzone lasts 0.15 My. Therefore, this allows us to constrain the age of the MCL between 124.97 ± 0.12 and 124.82 ± 0.12 Ma.

Micropaleontological and lithological evidence suggesting that MCL is an environmental signal

As described in the results, the MCL exhibits peculiar sedimentological features characterized by dark-colored sediment, alternating thin clay levels, laminated mudstones, massive mudstone and centimeter intervals showing millimeter-sized pebbly mudstones (Figs 2b, 3). In this layer, nannoconids and *Watznaueria* dominate the CN assemblages along with common pentaliths and *Assipetra*. The high abundance of nannoliths and heavily calcified coccoliths across different lithologies may reflect diagenetic overprinting. However, their specific paleoecological affinities provide meaningful paleoceanographic information for the MCL.

The ecology of *Watznaueria* has been widely debated (Roth & Krumbach, 1986; Erba, 1992, 1994; Williams & Bralower, 1995; Negri et al., 2003; Tremolada et al., 2006). However, this taxon is one of the most dissolution-resistant species and when the abundance of this taxon is > 40% (e.g., Thierstein, 1981; Thierstein & Roth, 1991; Williams & Bralower, 1995) it cannot be used as a trophic indicator, especially in the absence of small, dissolution prone, lightly calcified coccoliths such as *Biscutum constans*, *Zeugrhabdothus erectus* and *Diazomatholithus lehmanii.*

Nannoconids are the most abundant taxa of the assemblage with relative abundances comparable to the typical limestones of the Maiolica Fm. (Erba & Quadrio, 1987). Common nannoconids normally suggest oligotrophy (e.g., Busson & Noël, 1991; Coccioni et al., 1992; Erba, 1994; Herrle, 2003; Mutterlose & Bottini, 2013) and are typical of stable environments not influenced by continental inputs or upwelling. As indicated by Bersezio et al. (2002), lower abundance of nannoconids is found in black shales but this is not always true, as shown by the enrichment of nannoconids in some Tethyan Lower Cretaceous black shales investigated by Bréhéret (1983), Kennedy et al. (2000), Nagai et al. (2002), Herrle (2003) and in some upper lower Barremian black shales of the Boreal Realm (labeled Hauptblätterton or Munk-Marl Bed) described by Wulff et al. (2020). As inferred by Coccioni et al. (1992) and Erba (1994), nannoconids are considered analog of the modern species *Florisphaera profunda* Okada & Honjo, 1973, which inhabits the deep photic zone. Therefore, the abundance of this species should indicate that primary production occurred deep in the photic zone, likely in a deep chlorophyll maximum (DCM) as that invoked by Castradori (1993) for the sedimentation of the Quaternary Mediterranean sapropels and of the most recent Holocene S1 (10-6 ka). A DCM can develop following enhanced stratification of the water column and the formation of a low-salinity lid, which promotes the shoaling of the nutricline at the base of the photic zone. In this view, the relatively high abundance of pentaliths (*Micrantholithus* spp.) observed in the MCL (up to 16% of the association; Fig. 5) strongly supports this hypothesis (Parker et al., 1985; Siesser et al., 1992; Roth, 1994; Street & Bown, 2000; Bersezio et al., 2002; Bown, 2005; Bottini & Mutterlose, 2012; Quijano et al., 2012). Finally, *Assipetra* is a heavily calcified, dissolution-resistant form, generally common in our samples, especially in the lower interval of the MCL. Tremolada & Erba (2002) questioned the biogenic origin of this taxon and proposed its connection to specific nutrification events and/or physico-chemical reorganization of the mid-Cretaceous oceans. According to Tiraboschi & Erba (2010), *Rucinolithus*-*Assipetra* nannoliths were connected to manganese-rich carbonates and were interpreted as the result of hydrothermal emanations during rifting. They hypothesized that these nannoliths could be $CaCO_3$ inorganic precipitations and/or bacterial biocalcifications occurring under unusual physico-chemical oceanic conditions (i.e., igneous events, hydrothermal activity and worldwide anoxia). In any case, *Assipetra* remains a taxon with unclear paleoecological connections at the present level of research.

The study of calcareous nannoplankton reveals that the deposition of the MCL seems to have occurred under conditions of water stratification, due to the presence of low-salinity surface waters suggested by the dominance of deep dweller nannoconids and the high quantity of pentaliths. Similar to Quaternary sapropels (Castradori, 1993), these fresher waters would have uplifted the nutricline toward the base of the photic zone. This would have favored DCM formation and reduced vertical mixing, producing dysoxia-anoxia at the sea-bottom and allowing the preservation of OM (e.g., Föllmi, 2012; Martínez et al., 2020). However, we also have to consider that Bersezio et al. (2002), when addressing the origin of organic-rich layers in the Lombardian Maiolica Fm., stated that preservation of OM did not necessarily occur under anoxic conditions. On the contrary, they proposed that storage of OM probably resulted from enhanced terrestrial input of nutrients, siliciclastic, woody, and herbaceous fragments. This induced mesotrophic conditions and increased primary productivity. In any case, preservation of distinct sedimentary lamination occurs when benthic organisms do not operate sediment mixing and homogenization. In fact, except for specific benthic foraminifera adapted to anoxia (Glock et al., 2019), bioturbating organisms require oxygen; thus, lack of bioturbation results in lamination, which is a physical proxy indicating dysoxia/anoxia, as described in the well-studied pelagic successions of the Scaglia Bianca Fm. from the Belluno Basin and UMB by Gambacorta et al. (2016).

Deoxygenated conditions in the MCL are strongly supported by the high abundance of OM and the presence of fine-scale lamination, as revealed by mesoscale observations and petrographic analyses (Figs 2a and 6a-b). These features are consistent with dysoxic bottom-water conditions, plausibly related, as discussed, to prolonged water column stratification and bottom stagnation. In this context, we must explain how a re-sedimentation event, which interrupts the background sedimentation, occurred. Late Early Cretaceous normal faulting in different pelagic successions of the Western Tethys, characterized by a pelagic carbonate platform-basin system, is suggested by Cipriani & Bottini (2019); based on their evidence, we interpret the re-sedimentation interval as related to transport (debris flow) of early cemented clasts and unconsolidated matrix. This is possibly related to seismic trembling events, which may produce the very limited collapse of a superficial portion of the sediments on a slope, at least partly coherent. This determines a displacement of the content downwards where the unconsolidated sediments (matrix) and small pieces (clasts) of the more lithified portions flow. Nevertheless, this process did not cause reventilation of the sea-bottom as evidenced by the dark color of the sediment.

To explain water column stagnation and consequent deoxygenation episodes we must discuss their triggering mechanisms, which can be very heterogeneous (Matsumoto et al., 2022). In this view, episodes recorded in the Jurassic and Cretaceous are the result of two major mechanisms: 1) underwater volcanic activity that enhanced primary productivity and oxygen consumption at the bottom (like during OAE1a; e.g., Giraldo-Gomez et al., 2022) and contemporaneous weathering intensification related to climate warming (Gernon et al., 2024); 2) a phase of sea-level highstand associated with a stable, humid and warm climate, which increases continental runoff and fresh-waters discharge to the basins. These factors promote water-column stagnation, which in turn induces sea bottom deoxygenation (Martire, 1992). Regarding the first case, the Barremian represents a critical interval marked by a significant increase in volcanic activity on the Ontong Java Plateau, a large submarine igneous province in the equatorial western Pacific Ocean. Eruption ages range from approximately 128.2 to 119.6 Ma, with additional volcanic events occurring around 90 Ma. These submarine eruptions likely released substantial amounts of CO_2 and nutrients into the ocean, enhancing biological productivity and, in some cases, triggering widespread oceanic anoxia (Davidson et al., 2023). Such events contributed to global environmental instability, with notable lithological, biological, and chemostratigraphic impacts on the Tethyan realm. Mercury data, used as chemical proxy for volcanic activity, from the Subbetic domain suggest that volcanic pulses occurred during the ammonite Balearic Zone, approximately 375 kyr before the Faraoni Event, in the upper part of the Nicklesi Zone, approximately 500 kyr before the Mid-Barremian Event, and within the Taxy Event (Charbonnier et al., 2018). This indicates that in the case of MCL, which is younger, we can exclude the influence of volcanism. Instead, our petrographic analyses conducted on the laminated mudstones show evidence of sedimentary features such as peloids, abundant in the light laminae, and terrigenous minerals in the dark laminae (Fig. 7b). We interpret peloids as fecal pellets, formed in response to grazing and predation in the water column, particularly during periods of increased productivity. Terrigenous minerals, on the other hand, are likely due to aeolic and/or fluvial input into the basin (e.g., Mutterlose et al., 2009), settling in a calm, stagnant water column or reverse weathering affecting biosiliceous fossils (see Pellegrino et al., 2022). Furthermore, the cyclical alternation of peloids and terrigenous-rich laminae suggests seasonal climatic forcing with enhanced nutrient-driven productivity during cold/dry seasons and increased continental runoff during wet/warm seasons (Lees et al., 2004). On a longer timescale, the observed rhythmicity is consistent with a background paleoclimatic regime characterized by a warmer and wetter climate intensifying the hydrological cycle, similar to the three major episodes of widespread dysoxia that punctuated the late Hauterivian and Barremian sediments in the Western Tethys (the Faraoni, MBE and Taxy Events). Such conditions would enhance monsoonal precipitation or seasonal rainfall variability, amplifying sediment delivery and nutrient redistribution within the oceanic basin.

Another important point is the possible origin of continental inputs, including fresh waters and terrigenous material. Although the pelagic setting of the UMB during the Early Cretaceous might suggest a lack of continental influence on sedimentation processes, several lines of evidence, including the present study, indicate otherwise. Notably, Wouters et al. (2018) documented well-preserved continental material –such as woody parenchyma– in Barremian black shales at the Foce di Frontone section, located approximately 30 km northwest of the Mt. Cipollara section, stratigraphically above the Faraoni Level (uppermost Hauterivian). This provides clear evidence that organic continental inputs reached

Fig. 7 - (color online) Thin section photomicrographs and SEM images of freshly broken rock chips. a) Landscape view of the sediment texture showing the lamination in the lower portion, and scattered burrows (see arrows) associated with homogenous sediments. b) Enlargement of the lower portion of the landscape view showing undulate lamination made up of light laminae composed of peloid material (attributable to fecal pellet with average size of about 200 µm) and dark laminae showing silicate minerals. Note the alternation of laminated and massive portions. c) Reflected light photomicrograph showing the presence of radiolarians (c2) and calcite shells (c1). d) Transmitted light photomicrograph showing the radiolarians (see arrow) filled with calcite cement. e) Reflected light photomicrograph of the massive sample (MC3 BIS2) showing the clasts (black arrows). f) Reflected light photomicrograph of the massive sample MC -2 showing homogenous texture with radiolarians (black arrow) and calcite fossil shells. g) Back Scattering Electron SEM image showing phosphatic remains (g1) and framboidal pyrite (g2). h) SEM image of a freshly broken rock stub showing micrite and sparse and fragmented nannofossils. Scale bars correspond to 1 mm.

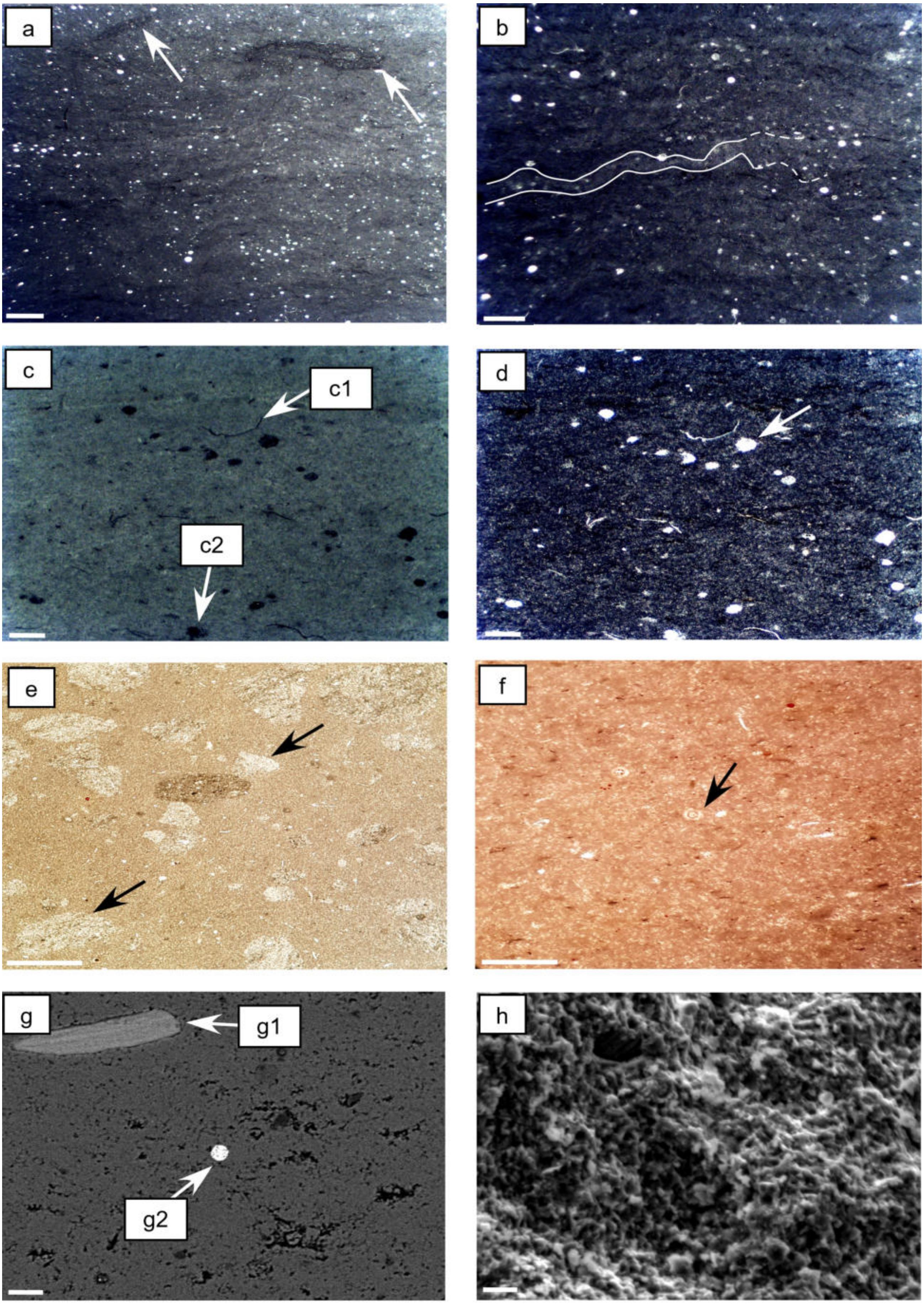
a
b
c
c1
c2
d
e
f
g
g1
g2
h

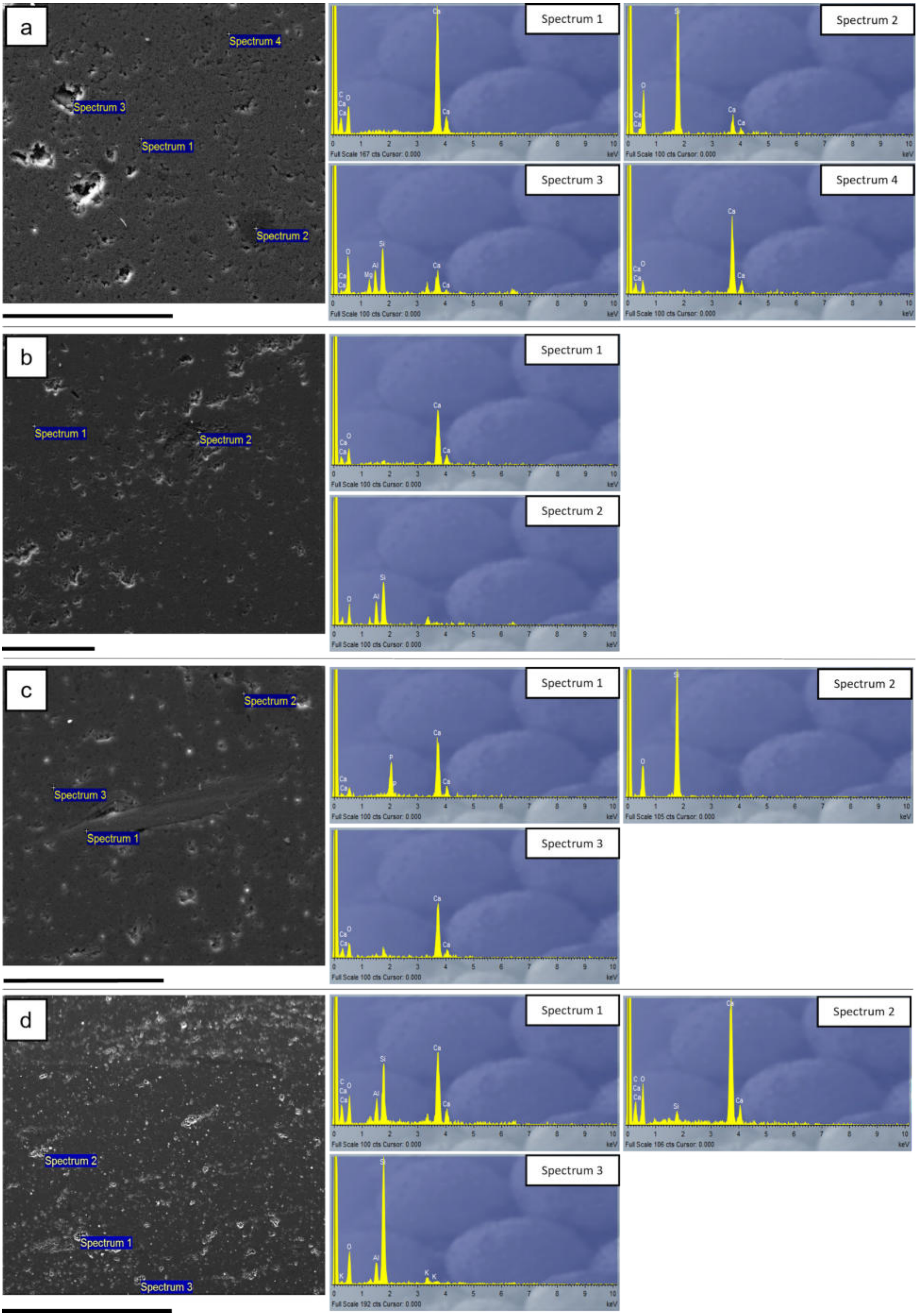
a
Spectrum 1
Spectrum 2
Spectrum 3
Spectrum 4
C
O
Ca
Si
Al
Mg
b
Spectrum 1
Spectrum 2
c
Spectrum 1
Spectrum 2
Spectrum 3
P
d
Spectrum 1
Spectrum 2
Spectrum 3
K
keV
Full Scale 167 cts Cursor: 0.000
Full Scale 100 cts Cursor: 0.000
Full Scale 105 cts Cursor: 0.000
Full Scale 106 cts Cursor: 0.000
Full Scale 192 cts Cursor: 0.000

the UMB during the Hauterivian-Barremian. Such inputs likely influenced the paleoecological conditions of the water column and may have contributed to the onset and development of environmental perturbations, including the MCL.

Similar to the deposition of Mediterranean sapropels, corresponding to positive sea level fluctuations in the pelagic environment (Capozzi & Picotti, 2003; Roveri & Taviani, 2003; Capozzi & Negri, 2009), we propose that the laminated, poorly oxygenated sediments characterizing the MCL are the result of a shift toward warmer and more humid climatic conditions, leading to increased precipitation on land, increased continental runoff and a short-term sea-level rise. During this short-term climate phase, increased precipitation, especially in the wet season, caused the recurring establishment of a strongly stratified water column above a DCM, as indicated by CN. The phase of sea-level highstand produced by this short-term climate regime may correspond to the relatively minor sea-level excursion (KBa2, less than 25 m; Haq, 2014) recorded in Western European basins.

Finally, regardless of the triggering mechanism of the paleoceanographic conditions discussed, rhythmic deoxygenation events, like those observed in the MCL, are widely reported in the Western Tethys domain during the Barremian (e.g., Bersezio et al., 2002; Bodin et al., 2006; Mutterlose et al., 2009; Föllmi et al., 2012) and can be interpreted as a gradual transition toward an unstable climatic system that characterizes the late Early Cretaceous (Aptian-Albian; Föllmi, 2012). The MCL can thus be interpreted as one of the climatic fluctuations that characterized the Tethyan regions during the Barremian with significant impacts on marine ecosystems.

Paleoecological and paleoenvironmental meaning of the ammonite assemblage

Based on the discussion above, it is crucial to understand whether environmental conditions impacted the ammonoid faunal assemblage and how the latter responded to these conditions.

The MCL showcases an ammonite faunal assemblage rich in heteromorphs and dominated by representatives of the Leptoceratoididae (Fig. 6). This concentration of Leptoceratoididae has not been previously documented within a single Maiolica Fm. bed in the UMB and remains poorly recorded even globally (Gőgös & Szives, 2024).

According to Reboulet et al. (2003, 2005), it is likely that heteromorph ammonites were more tolerant of variable environmental conditions than their planispiral counterparts. Zooplankton likely constituted their primary food source, as evidenced by jaw and radula morphology, as well as preserved remains of gastropods, crustaceans, and crinoids found within their body chambers (Wippich & Lehmann, 2004; Kruta et al., 2011; Hoffmann et al., 2021). These traits support the hypothesis of a predominantly planktonic lifestyle, potentially favored during periods of environmental perturbations associated with enhanced trophism in the water column.

Regarding Leptoceratoididae, several studies have attempted to reconstruct their ecology (Rieber, 1977; Vašíček & Wiedmann, 1994; Westermann, 1996; Lukeneder, 2003, 2015; Company et al., 2005; Gőgös & Szives, 2024). Early hypotheses proposed contrasting scenarios, ranging from a nectonic life above anoxic seafloors (Rieber, 1977) to inhabitation of coastal plains with algal mats (Vašíček & Wiedmann, 1994). However, more recent analyses –based on shell morphology, distribution, and faunal associations– tend to converge on a model supporting an epipelagic mode of life (Westermann, 1996; Cecca, 1998b; Company et al., 2005; Gőgös & Szives, 2024). The small, delicate shells of Leptoceratoididae suggest passive buoyancy and point to planktonic or pseudoplanktonic behavior. We agree with the interpretation of Gőgös & Szives (2024), who considered such adaptations consistent with life in the upper part of the water column, near or within the nutricline, where phytoplankton and nutrients are most concentrated.

The best-known Leptoceratoididae-rich intervals (Lukeneder, 2003, 2005; Gőgös & Szives, 2024) occur within the *M. moutonianum*-*T. vandenheckii* ammonite Zone, a time that coincides in some domains of the Central Tethys with the MBE (Coccioni et al., 2003). This event, although evidencing a serious problem of correlation in different areas (Sprovieri et al., 2006; Főzi & Janssen, 2009; Mutterlose et al., 2009; Price et al., 2011; Föllmi, 2012; Yilmaz et al., 2012; Aguado et al., 2014; Martinez et al., 2020; Talbi et al., 2021; Pictet et al., 2022), was marked by a warmer and more humid climate in adjacent continental regions, which likely enhanced freshwater discharge and nutrient runoff into marine basins, possibly triggering the adaptive radiation of small-sized ammonites (Gőgös & Szives, 2024).

It should be noted, however, that in the MCL, unlike the levels described by Lukeneder (2003, 2005) and Gőgös & Szives (2024), Leptoceratoididae represent 36% of the ammonite assemblages compared to values > 80% in the other cases. In the MCL, they dominate the assemblage but coexist with normal coiled ammonites. Following Reboulet et al. (2003, 2005) the normal coiling ammonites show higher abundances and dominate in oligotrophic, stable paleoenvironmental conditions, while heteromorphs were dominant in mesotrophic conditions, due to the availability of planktonic food and for the creation of shallower ecological niches.

Therefore we hypothesize that the co-occurrence of heteromorphic and normal coiled ammonites in the MCL could be explained by assuming two main scenarios: 1) variations in primary productivity, from oligotrophy to mesotrophy, occurred seasonally alternatively favoring normal coiling and heteromorphic forms, but we missed the signal due to the sampling resolution and sediment compaction; 2) ecological segregation due to water column stratification, a DCM enhanced primary productivity, providing favorable conditions for the concentration of Leptoceratoididae in the epipelagic domain while the

Fig. 8 - (color online) SEM images of the thin sections in Fig. 7 (left) showing selected points for EDS analysis. Corresponding EDS spectra and elemental compositions are reported on the right, highlighting the chemical characteristics of the analyzed samples. Scale bar for (a) and (c) correspond to 90 µm; scale bar for (b) corresponds to 100 µm; scale bar for (d) corresponds to 300 µm.

deeper layers (meso to bathy-pelagic domain) remained stable, supporting the persistence of oligotrophic, normal coiling forms.

Seasonal variations in primary productivity are supported by sedimentological evidence observed under SEM. The passive floating in the epipelagic environment of Leptoceratoididae (Westermann, 1996; Cecca, 1998b; Company et al., 2005; Gőgös & Szives, 2024) implies that these forms were adapted to the presence of a relatively stable DCM over time. Although the depth of the DCM likely shifted seasonally in response to climatic fluctuations, such variations would not have caused the cyclical appearance or disappearance of Leptoceratoididae, as might be expected in short-lived planktonic organisms. Instead, their longer life cycles (Kennedy & Cobban, 1976; Bucher et al., 1996) and limited ecological plasticity suggest occupation of a specific shallow niche. In contrast, normal coiling ammonites likely inhabited deeper, oligotrophic layers. This vertical ecological partitioning provides a more robust explanation for their stratigraphic co-occurrence than temporal alternation linked to seasonal productivity changes. Therefore, we suggest that the co-occurrence of heteromorphic and normal coiling forms within the MCL is best explained by ecological segregation driven by water column stratification (Fig. 9). Consequently, mass occurrences of Leptoceratoididae tend to be confined to specific stratigraphic intervals, such as the MCL, which reflect prolonged periods of stable water column stratification, even with seasonal variation. Instead, under stable oceanographic conditions –characterized by oligotrophy and a mixed water column– Leptoceratoididae are likely absent due to the lack of a sustained ecological niche suitable for their proliferation.

Finally, the near monospecific heteromorphic Leptoceratoididae association described in other black shales of comparable age (Rieber, 1977; Lukeneder, 2003, 2005; Gőgös & Szives, 2024) indicates more stable higher trophic conditions over time or a greater thickness of the water column affected by the increase in nutrients. This could be related to the more proximal location to emerged landmasses characterizing the other levels, where runoff is better expressed than in the distal epicontinental basin of the UMB.

In summary, environmental perturbations highlighted during the MCL deposition, have produced significant effects on ammonoid fauna. The MCL records an increase of plankton feeding planktonic forms, which proliferate in separate niches from their normal coiling counterparts. However, our interpretation aligns with the hypothesized Leptoceratoididae lifestyle.

Paleobiogeographic importance of the MCL

Although assemblages rich in leptoceratoids are poorly documented, single specimens have been found in many areas. In fact, Vašíček & Wiedmann (1994) consider their distribution to be worldwide. Leptoceratoididae are reported from Japan (Matsukawa, 1987, 1988) to the Caribbean (Karsten, 1858; Royo Y Gómez, 1945; Etayo-Serna, 1968; Myczyński, 1977; González-Arreola & Carillo-Martínez, 1986; Myczyński & Triff, 1986). However, their main distribution was on the southern shelf margin of the European Plate, from the Caucasian Basin in the east, to the Prebetic and Subbetic Basins in southern

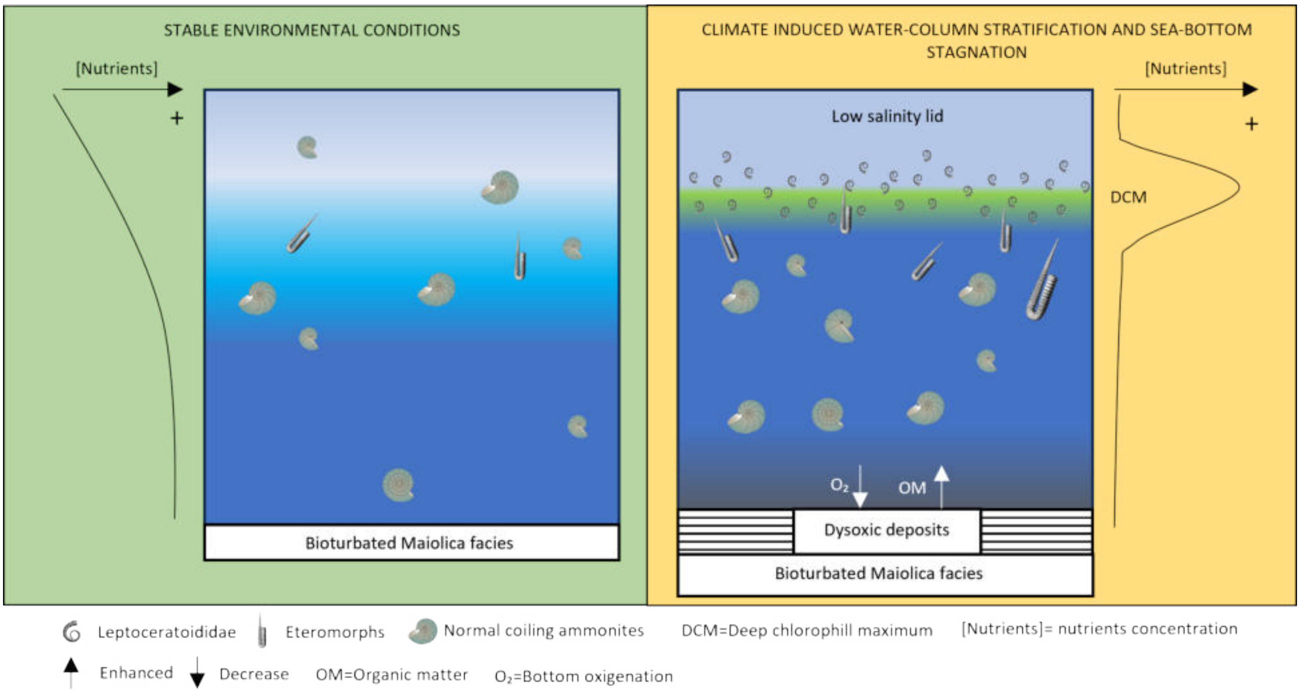

Fig. 9 - (color online) Conceptual vertical cross-section comparing two oceanographic scenarios to explain the stratigraphic co-occurrence of heteromorphic (Leptoceratoididae) and normally coiled ammonite taxa. The left panel represents ordinary conditions, characterized by a mixed, oligotrophic water column lacking a defined DCM. Under these conditions, Leptoceratoididae are likely absent due to the lack of their shallow ecological niche. The right panel illustrates stratified conditions inferred for the MCL, with a well-developed, seasonally dynamic DCM (green-shaded area) and dysoxia at the sea-bottom. The development of a shallow DCM supports the persistent presence of passively buoyant Leptoceratoididae. In these ecological settings normal coiled ammonites are interpreted to have inhabited deeper, oligotrophic layers.

Spain in the west (see Vašíček & Wiedmann, 1994 for a detail description of single areas). An exception to the abundance of Leptoceratoididae in this area is the northern margin of the African plate and particularly the Adria microplate (Apennines, Lombardy), between the African and European margins, where Leptoceratoididae are less abundant (Vašíček & Wiedmann, 1994), rare or practically absent according to Cecca (1998a). In fact, before this contribution, only singles specimens of Leptoceratoididae were reported in the northern margin of the African plate by Rieber (1977), Cecca et al. (1995), Cecca & Landra (2000) and Lukeneder (2012). The discovery of a high number of specimens of Leptoceratoididae from the MCL testifies that this family of ammonites was present and, in some cases, abundant also in the northern margin of the African plate. Since Leptoceratoids prospered in basinal environments with a dominance of clayey-marly facies (Vašíček & Wiedmann, 1994), like the southern shelf of the central European plate, the UMB was certainly favorable for these forms of r-strategist ammonites. Further studies in other sections and biozones will be essential to understand the real abundance of these forms in the area in question, which, moreover, could represent an evolutionary center for the Leptoceratoididae. This is suggested by the first appearance datum section of *L. ternbergense* in the lower *K. compressissima* Zone, so far described only in the *M. moutonianum* Zone of the Northern Calcareous Alps (Lukeneder, 2003, 2005). Thus, the Leptoceratoididae-rich MCL is a key for our knowledge of the paleobiogeographic distribution of this important ammonite family.

CONCLUSION

The picture that emerges from our integrated study on a peculiar lower Barremian black shale from the Umbria-Marche Maiolica Fm. suggests that its deposition occurred in oligo-mesotrophic, stable, salinity-stratified water masses caused by a climatic fluctuation. This fluctuation had effects on the continental freshwater supply to the UMB as well as on the production of OM, which contributed to generating intermittent oxygen-depleted conditions at the sea bottom. These conditions created new shallow ecological niches, favoring the Leptoceratoididae and allowing for their radiation, confirming recent paleoecological interpretations of this family. Interestingly, the ammonite assemblage in which heteromorphic (mesotrophic) forms occur with normal coiled (oligotrophic) forms suggests that the stratification of the water masses favored the coexistence of both (i.e., ecological segregation) and explains the paleontological record.

The Leptoceratoididae mass occurrence within the MCL, dated at the lower *K. compressissima* Zone of the lower Barremian, represents an episode of environmental change framed in a trend of progressive increase of OM-rich deposits in the UMB. With this contribution, we report the massive presence of Leptoceratoididae between the southern margin of the European plate and the northern margin of the African plate, where this family of ammonites was poorly documented. We also propose the UMB as a possible evolutionary center for Leptoceratoididae, as suggested by the first appearance datum section of the *L. ternbergense*. Further in-depth studies of these episodes, their onset mechanisms, their development, and their responses to the marine biota, will be fundamental for a better understanding of the events that characterized the Cretaceous in UMB.

SYSTEMATIC PALEONTOLOGY

In this section the taxonomic interpretations of the Leptoceratoididae found in the MCL are discussed.

Phylum Mollusca Linnaeus, 1758
Class Cephalopoda Cuvier, 1797
Order Ammonitida Haeckel, 1866
Superfamily Ancyloceratoidea Gill, 1871
Family Leptoceratoididae Thieuloy, 1966

Genus *Leptoceratoides* Thieuloy, 1966
Type species *Crioceras* (*Leptoceras*) *pumilum* Uhlig, 1883

Description - The genus *Leptoceratoides* is typically defined by its small size and crioconic shell shape, usually only a few centimeters in diameter (Vašíček & Wiedmann, 1994; Wright et al., 1996). The ribbing pattern is generally simple, although the orientation of the ribs can differ among species (Vašíček & Wiedmann, 1994; Wright et al., 1996). In some cases, such as in *L. balernaensis* Rieber, 1977, the direction, density, and thickness of the ribs may change during growth, as also seen in *L. subtilis* Uhlig, 1883 and *L. pumilus* Uhlig, 1883, resulting in an irregular rib pattern. One of the most distinctive features of the genus is the complete absence of ventrolateral tubercles or spines, clearly setting it apart from *Karsteniceras*.

Leptoceratoides ternbergense (Lukeneder in Lukeneder & Tanabe, 2002)
(Pl. 2, figs 1-6)

2002	*Karsteniceras ternbergense* Lukeneder, 2002 - Lukeneder & Tanabe, p. 18, Figs 3A-C, 4A-E.
2003	*Karsteniceras ternbergense* Lukeneder, 2002 - Lukeneder, p. 96, Pl. 10, figs 1-13.
2004	*Karsteniceras ternbergense* Lukeneder, 2002 - Lukeneder, p. 180, Pl. 3, fig. 2 (= Lukeneder, 2003, p. 96, Fig. 1).
2004	*Karsteniceras* cf. *ternbergense* Lukeneder, 2002 - Lukeneder, p. 44, Pl. 2, fig. 3.
2005	*Karsteniceras ternbergense* Lukeneder, 2002 - Lukeneder, p. 311, Fig. 6 (6-15).

Material - Sixteen internal moulds (Museum Codes: 4910 to 4925) in a moderate state of preservation. Most specimens are entire and show no fragmentation. Only two specimens (MC012BS and MC0013BS) are incomplete fragments. The specimens are observable on one side only. Due to mode of preservation, the suture line is not visible.

Description - Criocone shells showing trochospiral coiling. The sculpture comprises relatively dense, sharp and simple ribs. Some specimens show thick main ribs. Up to 45-50 single ribs are present on one whorl. No tubercles occur.

Discussion - The absence of nodules on the ventrolateral side rules out the possibility that the specimens belong to the genus *Karsteniceras*. The ribbing and the morphological pattern observed in our specimens are those typical of *L. ternbergense*, clearly distinguished from *L. pumilus* Uhlig, 1883 and *L. subtilis* Uhlig, 1883 based on the irregular rib pattern of the latters. Moreover, *L. pumilus* has biconcave, bifurcated ribs. *L. balernaense* Rieber, 1977 is distinguished for its sharper ribbing and the highest number of ribs per whorl.

Stratigraphic and geographic occurrence - In the UMB, *L. ternbergense* occurs in the lower *K. compressissima* Zone of the lower Barremian. Before these findings, *L. ternbergense* was reported only from the Northern Calcareous Alps of Austria, into the *M. moutonianum* Zone of lower Barremian. Our report represents the first appearance datum section of *L. ternbergense*.

Genus *Karsteniceras* Royo Y Gomez, 1945
Type species *Ancyloceras beyrichii* (Karsten, 1858)

Description - The genus *Karsteniceras* is generally characterized by tiny, few centimetres in diameter criocone morphology (Vašíček & Wiedmann, 1994; Wright et al., 1996), apart from *K. aequicostatum* Vašíček & Hoedemaeker, 2003b and ?*K. filicostatum* Stahlecker, 1935, which are bigger. The ribbing pattern is like *Leptoceratoides*; the major difference is the presence of ventrolateral tuberculation, which is the generic feature of *Karsteniceras*.

Karsteniceras ibericum Vašíček & Wiedmann, 1994
(Pl. 2, fig. 7)

1945 *Karsteniceras beyrichii* (Karsten, 1858) - Royo Y Gomez, p. 461, Pl. 71, fig. 1a-c.
1968 *Karsteniceras beyrichii* (Karsten, 1858) - Etayo-Serna, p. 54, Pl. 1, figs 1-3, Text-figs 4, 8-9.
1978 *Karsteniceras beyrichii* (Karsten, 1858) - Wiedmann, Pl. 4, fig. 2a-b.
1994 *Karsteniceras ibericum* Vašíček & Wiedmann, 1994 - Vašíček & Wiedmann, p. 212, Pl. 1, figs 4-5.
2024 *Karsteniceras ibericum* Vašíček & Wiedmann, 1994 - Gőgös & Szives, Pl. 6, figs 1, 3; Pl. 7, figs 1, 3; Pl. 8, figs 1, 3; Pl. 9, figs 1, 4; Pl. 10, figs 1, 5; Pl. 11, figs 1, 3.

Material - Two specimens (Museum Codes: 4926 and 4927), of which one complete (specimen MC025BS) and one fragmentated (specimen MC014BS). Both present moderate preservations. The specimens are observable on one side only. The suture line and ventral area are not visible.

Description - Small criocone specimens with dense ribbing in the body chamber. The latter appears predominantly rectiradiate, but few prorsiradiate ribs are present on the body chamber and rursiradiate ribs also appear near the opening. Small tuberculation is visible in the ventrolateral part of the phragmocone.

Discussion - Our specimens for the irregular rib pattern could resemble *K. beyrichii* (Karsten, 1858). Even if the distinguish between these two species is simple in well preserved and complete specimens, based on very different ventral areas, in our specimens ventral area is not visible. Despite that, in *K. beyrichii*, after a diameter of 20 mm, one or two stronger ribs alternate with bundles of one-four less pronounced ribs. In our specimens the ribs are of equal strength both in the body chamber and the phragmocone and suggest that the specimens belong to *K. ibericum*.

Stratigraphic and geographic occurrence - The species was described from the Western Tethyan region, primarily in the Iberian Peninsula (Sierra Mediana, Spain) and the Alps (Ranzenberg, Vorarlberg, Austria) (Wiedmann, 1978). In the Central Atlantic, it has been reported from Colombia, where it occurs in Barremian strata. In Austria, it was found near the boundary between the lower and upper Barremian, while in Spain, it is restricted to upper

---

EXPLANATION OF PLATE 1

(color online) Representative ammonite taxa within the MCL. All scale bars correspond to 1 cm. The specimens have been enlarged or reduced by a factor of x, as indicated for each specimen.

Fig. 1 - *Holcodiscus fallax* Spath, 1924. Lower interval of the MCL. Specimen no. MC009MAIB. 1.5x.

Fig. 2 - *Kotetishvilia compressissima* d'Orbigny, 1841. Lower interval of the MCL. Specimen no. MC007MAIB. 2.5x.

Fig. 3 - *Anahamulina* sp. Lower interval of the MCL. Specimen no. BO03BS. 2.5x.

Fig. 4 - *Anahamulina* cf. *lorioli* Uhlig, 1883. Lower interval of the MCL. Specimen no. MC016MAIB. 1x.

Fig. 5 - *Moutoniceras* sp. Lower interval of the MCL. Specimen no. MC015MAIB1. 1.2x.

Fig. 6 - *Lytoceras subfimbriatum* d'Orbigny, 1841. Lower interval of the MCL. Specimen no. MC013MAIB. 1x.

Fig. 7 - *Holcodiscus* aff. *nodosus* Karakash, 1907. Lower interval of the MCL. Specimen no. MC017MAIB. 3x.

Fig. 8 - *Astieridiscus* cf. *morleti* Kilian, 1889. Lower interval of the MCL. Specimen no. MC011MAIB. 2.5x.

Fig. 9 - Holcodiscidae indet. Nucleous of *Avramidiscus* sp.? Lower interval of the MCL. Specimen no. MC010MAIB1. 2.2x.

Fig. 10 - *Phyllopachiceras infundibulum* d'Orbigny, 1840. Lower interval of the MCL. Specimen no. MC014MAIB. 2.5x.

Fig. 11 - *Protetragonites* sp. Lower interval of the MCL. Specimen no. MC012MAIB. 2.5x.

Fig. 12 - *Barremites* sp. Lower interval of the MCL. Specimen no. MC0039BS. 2x.

1

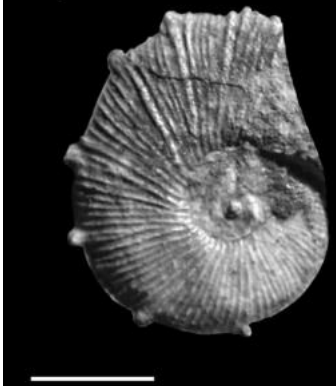

2

3

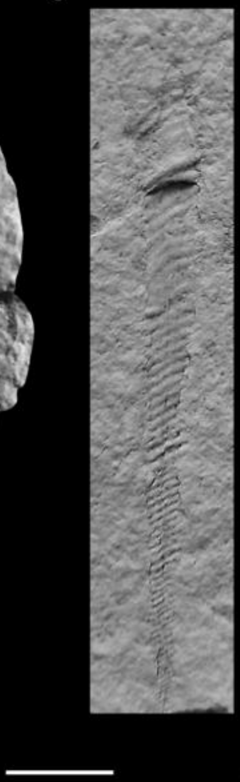

4

5

6

7

8

9

10

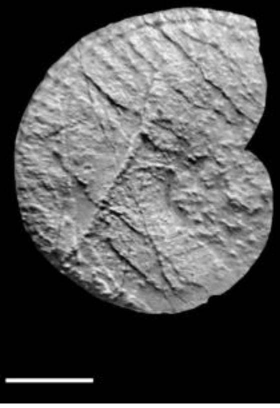

11

12

Barremian levels. The discoveries in Hungary (Gőgös & Szives, 2024) and Italy confirm the presence of the species in the early Barremian.

Karsteniceras beyrichoide Vašíček & Wiedmann, 1994
(Pl. 2, fig. 8)

1883 *Crioceras* (*Leptoceras*) *beyrichi* (Karsten, 1858) - Uhlig, p. 272, Pl. 32, figs 4, 6, ?8.
1960 *Leptoceras beyrichi* (Karsten, 1858) - Drushtchts, p. 295, Pl. 40, fig. 4.
1976 *Karsteniceras* aff. *beyrichi* (Karsten, 1858) - Avram, p. 34, Pl. 3, fig. 9.
1994 *Karsteniceras beyrichoide* Vašíček & Wiedmann - p. 213, Pl. 1, figs 6-8, Text-fig. 3A.
1998 *Karsteniceras beyrichoide* Vašíček & Wiedmann, 1994 - Vašíček & Klajmon, p. 334, Pl. 1, figs 12-14.
1999 *Karsteniceras beyrichoide* Vašíček & Wiedmann, 1994 - Vašíček, p. 220, Pl. 3, figs 4-5 (= Vašíček & Klajmon, 1998, Pl. 1, figs 12-13).

Material - A single specimen (Museum Code: 4928) moderately preserved, visible on a single side only.

Description - Small-sized criocone with trochospiral shell. The lateral sides are flat, as is the broad venter which carries a shallow siphonal furrow. Sculpture consists of single sharp ribs as broad as the intervals. Near the opening the rib became weak prorsiradiate. Marginal tubercles are present and show variable strength.

Discussion - The presence of ventrolateral tubercles suggests that this species belongs to the genus *Karsteniceras*. *Karsteniceras beyrichoide* resembles *K. beyrichii* but can be distinguished in its adult stage where the ribbing remains uniform, as clearly seen from our specimen. A further difference is that *K. beyrichii* has been described only from the Central Atlantic, in contrast to *K. beyrichoide*, which has been detected from the Silesian Unit, Outer Carpathians, Czech Republic. Doubtfully included are specimens from the Outer Dacidian Nappe, Romania, and from the Kuma River, North Caucasus (Vašíček & Wiedmann, 1994).

Stratigraphic and geographic occurrence - This species is reported by Vašíček & Wiedmann (1994) from the ?upper Barremian of the sites previously cited. In Central Apennines, *K. beyrichoide* is now reported from the lower *K. compressissima* Zone of the lower Barremian.

Karsteniceras sp. 1
(Pl. 2, figs 9-14)

Material - Twenty-two internal moulds (Museum Codes: 4929 to 4950), visible on a single side only.

Description - Regular crioconic coiling. The whorl section is rounded. The ribs are strong, straight or slightly rursiradiate, weaker along the umbilical margin, and become reinforced at the ventral area, forming small spines that are only sporadically observed due to the state of preservation of the specimens. The ribs originate from the very first whorls and remain consistent in spacing and strength throughout. The inter-rib spaces are wider than the ribs. In some specimens, two or three constrictions are present in the last whorl. In one specimen, a faint suture line is visible, showing a simple and well-developed L lobe. The E and U lobes are not observable.

Discussion - The specimens recovered can be attributed to the genus *Karsteniceras* due to the presence

---

EXPLANATION OF PLATE 2

(color online) Representative Leptoceratoididae within the MCL. The specimens have been enlarged or reduced by a factor of x, as indicated for each specimen.

Figs 1-6 - *Leptoceratoides ternbergense* Lukeneder, 2002. Lower interval of the MCL.
1 - Specimen no. MC008BS. 2x.
2 - Specimen no. MC009BS. 3.5x.
3 - Specimen no. MC010BS. 3.5x.
4 - Specimen no. MC011BS. 3.2x.
5 - Specimen no. MC012BS. 2x.
6 - Specimen no. MC034BS. 2.5x.

Fig. 7 - *Karsteniceras ibericum* Vašíček & Wiedmann, 1994. Lower interval of the MCL. Specimen no. MC014BS. 4x.

Fig. 8 - *Karsteniceras beyrichoide* Vašíček & Wiedmann, 1994. Lower interval of the MCL. Specimen no. MC001BS. 2.5x.

Figs 9-14 - *Karsteniceras* sp. 1. They are characterized by strong, rectiradiate ribs which end in a ventrolateral tubercle. The ventral area is not visible in any specimen as well as suture lines. The inter-ribs space is wide, and the ribs are spaced since the first whorls. In some specimens, the whorl section, from rounded to sub-rounded, undergoes reductions in diameter in some places of the shell. Lower interval of the MCL.
9 - Specimen no. MC015BS. 2.5x.
10 - Specimen no. MC019BS. 3x.
11 - Specimen no. MC017BS. 2x.
12 - Specimen no. MC018BS. 2x.
13 - Specimen no. MC024BS. 3x.
14 - Specimen no. MC020BS. 2.5x.

1

2

3

4

5

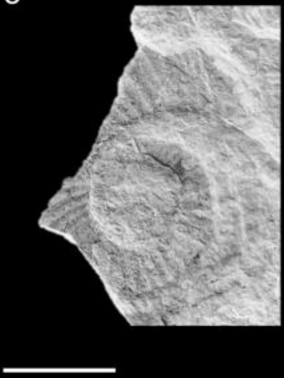

6

7

8

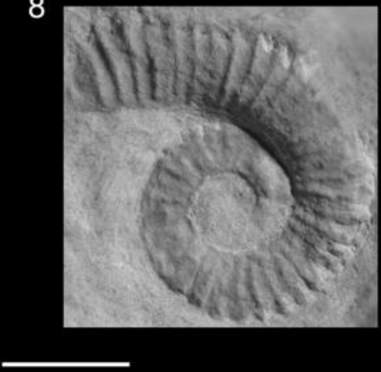

9

10

11

12

13

14

of ventrolateral tubercles. Owing to their strong and widely spaced ribbing, these forms may resemble *K. obatai* Matsukawa, 1987 but differ in that the latter exhibits three ontogenetic stages, during the first two of which the whorl grows in a cyrtoconic manner and lacks ornamentation. *Kasterniceras hoheneggeri* Vasicek & Wiedmann, 1994 may also resemble the recovered forms, particularly in terms of ribbing and the presence of grooves; however, in *K. hoheneggeri*, these grooves are restricted to the final half of the last whorl, unlike what is observed in the present specimens. Furthermore, *K. hoheneggeri* has thus far only been described from upper Barremian deposits (Vašíček & Wiedmann, 1994; Cecca & Landra, 2000). Similar ornamentation to our *Karsteniceras* sp. 1 is found in the specimens of *Karsteniceras* sp. 1 described by Gőgös & Szives (2024: pl. 12, figs 1-2). Further studies will be necessary to evaluate the conspecificity of the forms.

Stratigraphic and geographic occurrence - Specimens described come from the lower *K. compressissima* Zone of the lower Barremian of the UMB.

SUPPLEMENTARY ONLINE MATERIAL

Supplementary data of this work are available on the BSPI website at: https://www.paleoitalia.it/bollettino-spi/bspi-vol-643/

ACKNOWLEDGMENTS

The authors are indebted to Elisabetta Erba, Stefano Cresta, Alexander Lukeneder and Michael Company for the fruitful discussion leading to the first draft of the manuscript. Giovanna Della Porta is thanked for the stable isotope analyses, Caterina Morigi for providing the thin sections, Stefano Sassaroli for realizing the ammonite photos, Riccardo Cellocco for his help with cataloguing. The earlier draft benefitted from the comments from two anonymous reviewers and Ottilia Zsives.

REFERENCES

Aguado R., Company M., O'Dogherty L., Sandoval J. & Tavera J.M. (2014). Late Hauterivian–early Barremian calcareous nannofossil biostratigraphy, palaeoceanography, and stable isotope record in the Subbetic domain (southern Spain). *Cretaceous Research*, 49: 105-124.

Alvarez W. & Lowrie W. (1984). Magnetic stratigraphy applied to syn-sedimentary slumps, turbidites, and basin analysis-The Scaglia limestone at Furlo (Italy). *Geological Society of America Bulletin*, 95: 324-336.

Applegate J.L. & Bergen J.A. (1988). Cretaceous calcareous nannofossil biostratigraphy of sediments recovered from the Galicia Margin, ODP Leg 103. *In* Boillot G., Winterer E.L., et al. (eds), Proceedings of the Ocean Drilling Program, Scientific Results, Texas A & M University, Ocean Drilling Program, College Station, 103: 293-348.

Avram E. (1976). Nouvelles ammonites heteromorphes Bedouliennes du Couloir de la Dimbovicioara. *Memoires de l'Institut de Geologie et de Geophysique Bucarest*, 24: 75-82.

Barbera C. (1967). Ammoniti Giurassiche del Gran Sasso e dell'Aquilano. *Atti dell'Accademia delle Scienze Fisiche e Matematiche*, 6: 228-313.

Beltran C., De Rafélis M., Person A., Stalport F. & Renard M. (2009). Multiproxy approach for determination of nature and origin of carbonate micro-particles so-called "micarb" in pelagic sediments. *Sedimentary Geology*, 213: 64-76.

Bernoulli D. (1967). Probleme der sedimentation im Jura Westgriechenlands und des zentralen Apennin. *Verhandlungen der Naturforschenden Gesellschaft*, 78: 35-54.

Bersezio R., Erba E., Gorza M. & Riva A. (2002). Berriasian-Aptian black shales of the Maiolica formation (Lombardian Basin, Southern Alps, Northern Italy): local to global events. *Palaeogeography, Palaeoclimatology, Palaeoecology*, 180: 253-275.

Bertotti G., Picotti V., Bernoulli D. & Castellarin A. (1993). From rifting to drifting: Tectonic evolution of the South-Alpine upper crust from the Triassic to the Early Cretaceous. *Sedimentary Geology*, 86: 53-76.

Black M. (1971a). Coccoliths of the Speeton Clay and Sutterby Marl. *Proceedings of the Yorkshire Geological Society*, 38: 381-424.

Black M. (1971b). The systematics of coccoliths in relation to the paleontological record. *In* Funnell B.M. & Riedel W.R. (eds), The Micropaleontology of the Oceans. Cambridge University Press: 611-624.

Black M. (1973). British Lower Cretaceous Coccoliths. I-Gault Clay (Part 2). *Palaeontographical Society Monograph*, 127: 49-112.

Black M. & Barnes B. (1959). The structure of Coccoliths from the English Chalk. *Geological Magazine*, 96: 321-328.

Bodin S., Godet A., Föllmi K.B., Vermeulen J., Arnaud H., Strasser A., Fiet N. & Adatte T. (2006). The late Hauterivian Faraoni oceanic anoxic event in the western Tethys: evidence from phosphorus burial rates. *Palaeogeography, Palaeoclimatology, Palaeoecology*, 235: 245-264.

Bottini C. & Mutterlose J. (2012). Integrated stratigraphy of Early Aptian black shales in the Boreal Realm: calcareous nannofossil and stable isotope evidence for global and regional processes. *Newsletters on Stratigraphy*, 45: 115-137.

Bown P.R. (2005). Early to mid-Cretaceous calcareous nannoplankton from the northwest Pacific Ocean, ODP Leg 198, Shatsky Rise. *In* Bralower T.J., Premoli Silva I., et al. (eds), Proceedings of the Ocean Drilling Program, Scientific Results, Texas A & M University, Ocean Drilling Program, College Station, 198: 1096-2514.

Bown P.R. & Young J.R. (1998) Techniques. *In* Bown P.R. (ed.), Calcareous Nannofossil Biostratigraphy, Kluwer Academic Publishers, Dordrecht, Boston, London: 16-32.

Bown P.R., Rutledge D.C., Crux J.A. & Gallagher L.T. (1998). Lower Cretaceous. *In* Bown P.R. (ed.), Calcareous Nannofossil Biostratigraphy. Kluwer Academic Press, Dordrecht: 86-131.

Bréhéret J.G. (1983). Sur des niveaux de black shales dans l'Albien inférieur et moyen du domaine vocontien (SE de la France): étude de nannofaciès et signification des paléoenvironnements. *Bulletin du Muséum National d'Histoire Naturelle Paris*, 5: 113-159.

Breskovski S. (1977). Sur la classification de la famille Desmoceratidae Zittel, 1895 (Ammonoidea, Crétacé). *Comptes Rendu de l'Académie bulgare des Sciences*, 30: 891-894.

Brönnimann P. (1955). Microfossils incertae sedis from the Upper Jurassic and Lower Cretaceous of Cuba. *Micropaleontology*, 1: 28-51.

Bucher H., Landman N.H., Klofar S.M. & Guex J. (1996). Mode and rate of growth in ammonoids. *In* Landma N.H., Tanabe K. & Daws R.A. (eds), Ammonoid paleobiology. *Topics in Geobiology*, 13: 407-461.

Bukry D. (1969). Upper Cretaceous coccoliths from Texas and Europe. *University of Kansas Paleontological Contributions*, 51: 1-79.

Busson G. & Noël D. (1991). Les nannoconidés, indicateurs environnementaux des océans et mers épicontinentales du Jurassique terminal et du Crétacé inférieur. *Oceanologica Acta*, 14: 333-356.

Canavari M. (1878). Cenni geologici sul camerinese e particolarmente su di un lembo Titonico nel M. Sanvicino. *Bollettino del Regio Comitato Geologico d'Italia*, 9: 488-498.

Capozzi R. & Negri A. (2009). Role of sea-level forced sedimentary processes on the distribution of organic carbon-rich marine sediments: A review of the Late Quaternary sapropels in the Mediterranean Sea. *Palaeogeography, Palaeoclimatology, Palaeoecology*, 273: 249-257.

Capozzi R. & Picotti V. (2003). Pliocene sequence stratigraphy, climatic trends and sapropel formation in the Northern Apennines (Italy). *Palaeogeography, Palaeoclimatology, Palaeoecology*, 190: 349-371.

Castradori D. (1993). Calcareous nannofossils and the origin of eastern Mediterranean sapropels. *Paleoceanography*, 8: 459-471.

Cecca F. (1985). Alcune ammoniti provenienti dalla "Maiolica" dell'Appennino Centrale (Umbria, Marche e Sabina). *Bollettino del Servizio geologico d'Italia*, 103: 133-162.

Cecca F. (1998a). Early Cretaceous (pre-Aptian) ammonites of the Mediterranean Tethys: palaeoecology and palaeobiogeography. *Palaeogeography, Palaeoclimatology, Palaeoecology*, 138: 305-323.

Cecca F. (1998b). Hypotheses about the role of the trophism in the evolution of uncoiled ammonites: the adaptive radiations of the Ancyloceratina (Ammonoidea) at the end of the Jurassic and in the Lower Cretaceous. *Rendiconti Lincei. Scienze Fisiche e Naturali*, 9: 213-226.

Cecca F. & Landra G. (1994). Late Barremian-Early Aptian ammonites from the Maiolica Formation Near Cesana Brianza (Lombardy Basin, Northen Italy). *Rivista Italiana di Paleontologia e Stratigrafia*, 100: 395-422.

Cecca F. & Pallini G. (1996). Latest Hauterivian - Barremian ammonite biostratigraphy in the Umbria-Marche Apennines (Central Italy). *In* Bulot L. & Arnaud H. (eds), Lower Cretaceous Cephalopod Biostratigraphy of the western Tethys: Recent developments, regional synthesis and outstanding problems. *Geologie Alpine*, special volume 20: 205-217.

Cecca F., Marini A., Pallini G., Baudin F. & Begouen V. (1994). A guide-level of uppermost Hauterivian (Lower Cretaceous) in the pelagic succession of Umbria-Marche Apennines (Central Italy): the Faraoni Level. *Rivista Italiana di Paleontologia e Stratigrafia*, 99: 551-568.

Cecca F., Faraoni P., Marini A. & Pallini G. (1995). Field-trip across the representative sections for the Upper Hauterivian-Barremian ammonite biostratigraphy in the Maiolica exposed at Monte Nerone, Monte Petrano and Monte Catria (Umbria-Marche Apennines). *Memorie descrittive della Carta Geologica d'Italia*, 51: 187-211.

Centamore E., Chiocchini M., Deiana G., Micarelli A. & Pieruccini U. (1971). Contributo alla conoscenza del Giurassico dell'Appennino Umbro-Marchigiano. *Studi Geologici Camerti*, 1: 7-89.

Charbonnier G., Godet A., Bodin S., Adatte T. & Föllmi K.B. (2018). Mercury anomalies, volcanic pulses, and drowning episodes along the northern Tethyan margin during the latest Hauterivian-earliest Aptian. *Palaeogeography, Palaeoclimatology, Palaeoecology*, 505: 337-350.

Cipriani A. (2016). Geology of the Mt. Cosce sector (Narni Ridge, Central Apennines, Italy). *Journal of Maps*, 12: 328-340.

Cipriani A. & Bottini C. (2019). Early Cretaceous tectonic rejuvenation of an Early Jurassic margin in the Central Apennines: The "Mt. Cosce Breccia". *Sedimentary Geology*, 387: 57-74.

Coccioni R., Erba E. & Premoli-Silva I. (1992). Barremian-Aptian calcareous plankton biostratigraphy from the Gorgo Cerbara section (Marche, central Italy) and implications for plankton evolution. *Cretaceous Research*, 13: 517-537.

Coccioni R., Galeotti S. & Sprovieri M. (2003). The Mid-Barremian Event (MBE): the Prelude to the OAE1a. *American Geophysical Union, Fall Meeting 2003*: PP41B-0835.

Colacicchi R., Passeri L. & Pialli G. (1970). Nuovi dati sul Giurese umbro marchigiano ed ipotesi per un suo inquadramento regionale. *Memorie della Società Geologica Italiana*, 9: 839-874.

Company M., Aguado R., Sandoval J., Tavera J.M., Jimenez de Cisneros C. & Vera J.A. (2005). Biotic changes linked to a minor anoxic event (Faraoni Level, latest Hauterivian, Early Cretaceous). *Palaeogeography, Palaeoclimatology, Palaeoecology*, 224: 186-199.

Cook H.E. & Egbert R.M. (1979). Diagenesis of deep-sea carbonates. *Developments in Sedimentology*, 25: 213-288.

Covington J.M. & Wise S.W. (1987). Calcareous nannofossil biostratigraphy of a Lower Cretaceous deep-sea fan complex: Deep Sea Drilling Project Leg 93 Site 603, lower continental rise off Cape Hatteras. *In* van Hinte J.E., Wise S.W., et al. (eds), Initial Reports of the Deep Sea Drilling Project, Texas A & M University, Ocean Drilling Program, College Station, 93: 617-660.

Cuvier G. (1797). Tableau èlèmentaire de l'Histoire naturelle des animaux. 302 pp. Imprimeur Baudouin, Paris.

Davidson P.C., Koppers A.A., Sano T. & Hanyu T. (2023). A younger and protracted emplacement of the Ontong Java Plateau. *Science*, 380: 1185-1188.

De Lapparent J. (1931). Sur les prétendus "embryons" de Lagena. *Compte Rendu Sommaire des Séances de la Société Géologique de France*, 15: 222-223.

Deflandre G. (1953). Hétérogénéité intrinsèque et pluralité des éléménts dans les coccolithes actuels et fossiles. *Comptes rendus hebdomaire de l'Académie des sciences*, 237: 1785-1787.

Deflandre G. (1963). Sur les Microrhabdulidés, famille nouvelle de nannofossiles calcaires. *Comptes rendus hebdomaire de l'Académie des sciences*, 256: 3484-3487.

Deflandre G. & Fert C. (1954). Observations sur les coccolithophoridés actuels et fossiles en microscopie ordinaire et électronique. *Annales de Paléontologie*, 40: 115-176.

Deres F. & Achéritéguy J. (1980). Biostratigraphie des Nannoconides. *Bulletin des Centres de Recherches Exploration-Production Elf-Aquitaine*, 4: 1-53.

d'Orbigny A.D. (1840). Paléontologie française: Terrains Crètacès. Céphalopodes, 1: 1-120.

d'Orbigny A.D. (1841). Paléontologie française: Terrains Crètacès. Céphalopodes, 1: 121-430.

d'Orbigny A.D (1850). Podrome de paléontologie stratigraphique universelle des animaux mollusques & rayonnés faisant suite au cours élémentaire de paléontologie et de géologie stratigraphiques, 2: 1-189.

Douvillè H. (1890). Sur la classification des Cératites de la Craie. *Bulletin de la Société Géologique de France*, 18: 275-292.

Erba E. (1992). Calcareous nannofossil distribution in pelagic rhythmic sediments (Aptian-Albian Piobbico core, central Italy). *Rivista Italiana di Paleontologia e Stratigrafia*, 97: 455-484.

Erba E. (1994). Nannofossils and superplumes: the early Aptian "nannoconid crisis". *Paleoceanography*, 9: 483-501.

Erba E. (2004). Calcareous nannofossils and Mesozoic oceanic anoxic events. *Marine Micropaleontology*, 52: 85-106.

Erba E. & Quadrio B. (1987). Biostratigrafia a nannofossili calcarei, calpionellidi e foraminiferi planctonici della Maiolica (Titoniano superiore-Aptiano) nelle Prealpi Bresciane (Italia settentrionale). *Rivista Italiana di Paleontologia e Stratigrafia*, 93: 3-108.

Etayo-Serna F. (1968). Apuntaciones acerca de algunas amonitas interesantes del Hauteriviano y del Barremiano de la region de Villa de Leiva (Boyaca, Colombia, S.A.). *Boletin Geologico de la Universidad de Santander*, 24: 51-70.

Fabbi S. (2015). Geology and Jurassic paleogeography of the Mt. Primo-Mt. Castel Santa Maria ridge and neighbouring areas (Northern Apennines, Italy). *Journal of Maps*, 11: 645-663.

Fabbi S. & Santantonio M. (2012). Footwall progradation in synrift carbonate platform-slope systems (Early Jurassic, Northern Apennines, Italy). *Sedimentary Geology*, 281: 21-34.

Fabbi S., Citton P., Romano M. & Cipriani A. (2016). Detrital events within pelagic deposits of the Umbria-Marche basin (Northern Apennines, Italy). Further evidence of Early Cretaceous tectonics. *Journal of Mediterranean Earth Sciences*, 8: 39-52.

Faraoni P., Marini A. & Pallini G. (1998). The Hauterivian ammonite succession in the Central Apennines, Maiolica formation (Petrano Mt., Cagli - PS): preliminary results. *Palaeopelagos*, 5: 227-236.

Farinacci A., Mariotti N., Nicosia U., Pallini G. & Schiavinotto F. (1981). Jurassic sediments in the Umbro-Marchean Apennines: An alternative model. *In* Farinacci A. & Elmi S. (eds), Proceedings of Rosso Ammonitico Symposium Roma, Edizioni Tecnoscienza: 335-398.

Föllmi K.B. (2012). Early Cretaceous life, climate and anoxia. *Cretaceous Research*, 35: 230-257.

Föllmi K.B., Bôle M., Jammet N., Froidevaux P., Godet A., Bodin S., Adatte T., Matera V., Fleitmann D. & Spangenberg J.E. (2012). Bridging the Faraoni and Selli oceanic anoxic events: late Hauterivian to early Aptian dysaerobic to anaerobic phases in the Tethys. *Climate of the Past*, 8: 171-189.

Főzy I. & Janssen N.M.M. (2009). Integrated Lower Cretaceous biostratigraphy of the Bersek Quarry, Gerecse Mountains, Transdanubian Range, Hungary. *Cretaceous Research*, 30: 78-92.

Galluzzo F. & Santantonio M. (2002). The Sabina Plateau: a new element in the Mesozoic palaeogeography of Central Apennines. *Bollettino della Società Geologica Italiana*, volume speciale 1: 561-588.

Gambacorta G., Bersezio R., Weissert H. & Erba E. (2016). Onset and demise of Cretaceous oceanic anoxic events: The coupling of surface and bottom oceanic processes in two pelagic basins of the western Tethys. *Paleoceanography*, 31: 732-757.

Gernon T.M., Mills B.J.W., Hincks T.K., Merdith A.S., Alcott L.J., Rohling E.J. & Palmer M.R. (2024). Solid Earth forcing of Mesozoic oceanic anoxic events. *Nature Geosciences*, 17: 926-935.

Gill T. (1871). Arrangement of the families of mollusks. Prepared for the Smithsonian Institution. *Smithsonian Miscellaneous Collections*, 227: 17-49.

Giraldo-Gómez V.M., Petrizzo M.R., Erba E. & Bottini C. (2022). Paleoceanographic inferences from benthic foraminifera across the early Aptian Ocean Anoxic Event 1a in the western Tethys. *Palaeogeography, Palaeoclimatology, Palaeoecology*, 588: 110803.

Glock N., Roy A.S., Romero D., Wein T., Weissenbach J., Revsbech N.P., Høgslund S., Clemens D., Sommer S. & Dagan T. (2019). Metabolic preference of nitrate over oxygen as an electron acceptor in foraminifera from the Peruvian oxygen minimum zone. *Biological Sciences*, 116: 2860-2865.

Gőgös G. & Szives O. (2024). First report of the Mid Barremian Event from the Transdanubian Range (Hungary) and associated Leptoceratoididae (Ammonoidea) fauna. *Hungarian Geological Society*, 154: 199-238.

González-Arreola C. & Carillo-Martinez M. (1987). Amonitas del Jurasico superior (Titoniano superior) y del Cretacico inferior (Hauteriviano-Barremiano) del area de San Joaquin-Vizarron, Estado de Queretaro. *Universidad National Autonoma de Mexico, Instituto de Geologia, Revista*, 6: 171-177.

Górka H. (1957). Les Coccolithophoridés du Maestrichtien supérieur de Pologne. *Acta Palaeontologica Polonica*, 2: 239-284.

Haeckel E. (1866). Generelle Morphologie der Organismen: Allgemeine Grundzüge der organischen Formen-Wissenschaft, mechanisch begründet durch die von Charles Darwin reformierte Descendenz-Theorie. Band 1: Allgemeine Anatomie. Band 2: Allgemeine Entwicklungsgeschichte:1-160.

Haq B.U. (2014). Cretaceous eustasy revisited. *Global and Planetary Change*, 113: 44-58.

Herrle J.O. (2003). Reconstructing nutricline dynamics of mid-Cretaceous oceans: evidence from calcareous nannofossils from the Niveau Paquier black shale (SE France). *Marine Micropaleontology*, 47: 307-321.

Hoffmann R., Slattery J.S., Kruta I., Linzmeier B.J., Lemanis R.E., Mironenko A., Goolaerts S., De Baets K., Peterman D.J. & Klug C. (2021). Recent advances in heteromorph ammonoid palaeobiology. *Biological Reviews*, 96: 576-610.

Hyatt A. (1900). Cephalopoda. *In* Zittel A. (ed.), *Texbook of Paleontology*, London, Macmillan: 502-592.

Kamptner E. (1931). *Nannoconus steinmanni* novo gen., novo spec., ein merkwurdiges gesteinbildendes Mikrofossil aus dem jungeren Mesozoikum der Alpen. *Paläontologische Zeitschrift*, 13: 288-298.

Karakash N.I. (1907). Nizhne-melovye odozheniia Kryma i ikh fauna (The Lower Cretaceous of the Crimea and its fauna). *Trudy imperatorskogo S.-Peterburgskogo Obshchstva Estestvoispytatelei*, 32: 1-482.

Karsten H. (1858). Uber die geognostischen Verhaltnisse des westlichen Columbien, der heutigen Republiken Neu-Granada und Equator. *Amtliche Benchte, Versammlung Deutscher Naturforscher und Arzte*, 32: 80-117.

Kennedy W.J. & Cobban W.A. (1976). Aspects of ammonite biology, biogeography, and biostratigraphy. *Special Papers in Palaeontology*, 17: 1-82.

Kennedy W.J., Gale A.S., Bown P.R., Caron M., Davey R.J., Gröcke D. & Wray D.S. (2000). Integrated stratigraphy across the Aptian-Albian boundary in the Marnes Bleues, at the Col de Pré-Guittard, Arnayon (Drôme), and at Tartonne (Alpes-de-Haute-Provence), France: a candidate Global Boundary Stratotype Section and Boundary Point for the base of the Albian Stage. *Cretaceous Research*, 21: 591-720.

Kilian C.C.C.W. (1889). Sur quelques fossiles nouveaux on peu connus du Crétacé inférieur de la Provence. *Bulletin de la Société Géologique de France*, 3: 663-691.

Kilian C.C.C.W. (1910). Sur l'origine du groupe de l'Ammonites percevali Uhlig du Barremien. *Bulletin de la Société Géologique de France*, 4: 7.

Klein J., Busnardo R., Company M., Delanoy G., Kakabadze M., Reboulet S., Ropolo P., Vasícek Z. & Vermeulen J. (2007). Bochiantitoidea, Protancyloceratoidea, Ancyloceratoidea, Ptychoceratoidea. *In* Riegraf W. (ed.), Fossilium Catalogus III: Animalia, Blackhuys, Leiden, 144: 1-381.

Kruta I., Landman N., Rouget I., Cecca F. & Tafforeau P. (2011). The role of ammonites in the Mesozoic marine food web revealed by jaw preservation. *Science*, 331: 70-72.

Lees J.A., Bown P.R., Young J.R. & Riding J.B. (2004). Evidence for annual records of phytoplankton productivity in the Kimmeridge Clay Formation coccolith stone bands (Upper Jurassic, Dorset, UK). *Marine Micropaleontology*, 52: 29-49.

Linnaeus C. (1758). Systema Naturae per Regna Tria Naturae, secundum Classes, Ordines, Genera, Species cum characteribus, differentiis; synonymis, locis. Editio Decima, reformata. 823 pp. Laurentii Salvii, Stockholm.

Lory P. (1898). Le Crétacé inférieur du Dévolvy et des regions voisines. *Bulletin de la Société Géologique de France*, 3: 132-138.

Lukeneder A. (2003). The Karsteniceras Level: Dysoxic Ammonoid Beds within the Early Cretaceous (Barremian, Northern Calcareous Alps, Austria). *Facies*, 49: 87-100.

Lukeneder A. (2005). An equivalent of the Karsteniceras level within the Vienna woods (Sparbach section, Lunz nappe, northern calcareous Alps, Lower Austria). *Geologica Carpathica*, 56: 307-315.

Lukeneder A. (2012). New biostratigraphic data on an Upper Hauteriviane-Upper Barremian ammonite assemblage from the Dolomites (Southern Alps, Italy). *Cretaceous Research*, 35: 1-21.

Lukeneder A. (2015). Ammonoid Habitats and Life History. *In* Klug C., Korn D., De Baets K., Kruta I. & Mapes R. (eds), Ammonoid Paleobiology: From anatomy to ecology. *Topics in Geobiology*, 43: 689-791.

Lukeneder A. & Tanabe K. (2002). In situ finds Aptychi in the Barremian of Alpine Lower Cretaceous (Barremian, Northen Calcareous Alps, Upper Austria). *Cretaceous Research*, 23: 15-24.

Manivit H. (1966). Sur quelques coccolithes nouveaux du Néocomien. *Compte Rendu Sommaire des Séances de la Société Géologique de France*, 7: 267-268.

Martinez M., Aguardo R., Company M., Sandoval J. & O'Dogherty L. (2020). Integrated astrochronology of the Barremian Stage (Early Cretaceous) and its biostratigraphic subdivisions. *Global and Planetary Change*, 195: 103368.

Martire L. (1992). Sequence stratigraphy and condensed pelagic sediments. An example from the Rosso Ammonitico Veronese, northeastern Italy. *Palaeogeography, Palaeoclimatology, Palaeoecology*, 94: 169-191.

Matsukawa M. (1987). Early shell morphology of *Karsteniceras* (ancyloceratid) from the Lower Cretaceous Choshi Group, Japan and its significance to the phylogeny of Cretaceous heteromorph ammonites. *Transactions and Proceedings of the Palaeontological Society of Japan*, 148: 346-359.

Matsukawa M. (1988). Barremian ammonites from the Ishido Formation, Japan - supplements and faunal analysis. *Transactions and Proceedings of the Palaeontological Society of Japan*, 149: 396-416.

Matsumoto H., Coccioni R., Frontalini F., Shirai K., Jovane L., Trindade R., Savian J.F. & Kuroda J. (2022). Mid-Cretaceous marine Os isotope evidence for heterogeneous cause of oceanic anoxic events. *Nature Communications*, 13: 239.

Menichetti M. (2016). Early Cretaceous tectonic event in the Adria: Insight from Umbria-Marche pelagic basin (Italy). *In* Menichetti M., Coccioni R. & Montanari A. (eds), The Stratigraphic Record of Gubbio: Integrated Stratigraphy of the Late Cretaceous–Paleogene Umbria-Marche Pelagic Basin. *Geological Society of America, Special Paper* 524: 35-55.

Mutterlose J. & Bottini C. (2013). Early Cretaceous chalks from the North Sea giving evidence for global change. *Nature Communications*, 4: 1686.

Mutterlose J., Pauly S. & Steuber T. (2009). Temperature controlled deposition of early Cretaceous (Barremian–early Aptian) black shales in an epicontinental sea. *Palaeogeography, Palaeoclimatology, Palaeoecology*, 273: 330-345.

Myczyński R. (1977). Lower Cretaceous ammonites from Sierra del Rosario (Western Cuba). *Acta Palaeontologica Polonica*, 22: 139-173.

Myczyński R. & Triff J. (1986). Los ammonites del Cretacico Inferior de las provincias de Pinar del Rio y Matanzas. *Bulletin of the Polish Academy of Sciences, Earth Sciences*, 34: 113-137.

Nagai K., Furukawa M., Yoshiyama T., Yoshida T., Giraud F., Inagaki F., Nishi H., Sakamoto T. & Okada H. (2002). High-resolution analysis of calcareous nannofossils from OAE1 sequences exposed in SE France. *Journal of Nannoplankton Research*, 24: 141.

Negri A., Cobianchi M., Luciani V., Fraboni R., Milani A. & Claps M. (2003). Tethyan Cenomanian pelagic rhythmic sedimentation and Pleistocene Mediterranean sapropels: is the biotic signal comparable?. *Palaeogeography, Palaeoclimatology, Palaeoecology*, 190: 373-397.

Noël D. (1959). Étude de coccolithes du Jurassique et du Crétacé inférieur. *Publications du Service de la Carte Géologique de l'Algérie Bulletin*, 20: 155-196.

Noël D. (1965). Sur les Coccolithes du Jurassique Européen et d'Afrique du Nord. Essai de classification des coccolithes fossiles. *Éditions du Centre National de la Recherche Scientifique*: 1-209.

Noël D. & Melguen M. (1978). Nannofacies of Cape Basin and Walvis Ridge sediments, lower Cretaceous to Pliocene. *In* Bolli H.M., Ryan W.B.F. et al. (eds), Initial Reports of the Deep Sea Drilling Project, Texas A & M University, Ocean Drilling Program, College Station, 40: 487-524.

Okada H. & Honjo S. (1973). The Distribution of Oceanic Coccolithophores in the Pacific. *Deep Sea Research*, 20: 355-374.

Olòriz F. (1990). Ammonite phenotypes and Ammonite distributions. Notes and comments. *In* Pallini G., Cecca F., Cresta S. & Santantonio M. (eds), Atti II Convegno Fossili, Evoluzione, Ambiente (Pergola): 417-426.

Olòriz F., Rodriguez-Tovar F.J., Marques B. & Caraquel E.G. (1993). Ecostratigraphy and sequence stratigraphy in high frequency sea level fluctuations: examples from Jurassic macroinvertebrate assemblages. *Palaeogeography, Palaeoclimatology, Palaeoecology*, 101: 131-145.

Parker M.E., Clark M. & Wise S.W. Jr. (1985). Calcareous nannofossils of Deep Sea Drilling Project Sites 558 and 563, North Atlantic Ocean: biostratigraphy and the distribution of Oligocene braarudosphaerids. *In* Bougault H., Cande S.C. et al. (eds), Initial Reports of the Deep Sea Drilling Project, Texas A & M University, Ocean Drilling Program, College Station, 82: 559-589.

Pellegrino L., Natalicchio M., Birgel D., Pastero L., Carnevale G., Jordan R.W., Peckmann J., Zanellato N. & Dela Pierre F. (2022). From biogenic silica and organic matter to authigenic clays and dolomite: Insights from Messinian (upper Miocene) sediments of the Northern Mediterranean. *Sedimentology*, 70: 505-537.

Perch-Nielsen K. (1979). Calcareous nannofossils from the Cretaceous between the North Sea and the Mediterranean. *In* Wiedmann J. (ed.), Aspekte der Kreide Europas. *International Union Geological Sciences*, 6: 223-272.

Perch-Nielsen K. (1985). Mesozoic calcareous nannofossils. *In* Bolli H.M., Saunders J.B. & Perch-Nielsen K. (eds), Plankton Stratigraphy. Cambridge University Press: 329-426.

Pictet A., Kürsteiner P. & Tschanz K. (2022). Record of a dense succession of drowning phases in the Alpstein Mountains, north-eastern Switzerland: Part I-the Lower Cretaceous Tierwis Formation (latest Hauterivian to latest Barremian). *Swiss Journal of Geosciences*, 115: 1-31.

Pierantoni P., Deiana G. & Galdenzi S. (2013). Stratigraphic and structural features of the Sibillini Mountains (Umbria Marche Apennines, Italy). *Italian Journal of Geosciences*, 132: 497-520.

Price G.D., Főzy I., Janssen N.M.M. & Pálfy J. (2011). Late Valanginian–Barremian (Early Cretaceous) palaeotemperatures inferred from belemnite stable isotope and Mg/Ca ratios from Bersek Quarry (Gerecse Mountains, Transdanubian Range, Hungary). *Palaeogeography, Palaeoclimatology, Palaeoecology*, 305: 1-9.

Quijano M.L., Castro J.M., Pancost R.D., De Gea G.A., Najarr M., Aguado R. & Martín-Chivelet J. (2012). Organic geochemistry, stable isotopes, and facies analysis of the Early Aptian OAE—New records from Spain (Western Tethys). *Palaeogeography, Palaeoclimatology, Palaeoecology*, 365: 276-293.

Ramaccioni G. (1939). Fauna Giurassica e Cretacea di Monte Cucco e dintorni (Appennino centrale). *Palaeontographia Italica*, 9: 143-214.

Reboulet S. & Atrops F. (1995). Rôle du climat sur les migrationset la composition des peuplements d'ammonites du Valanginien supérieur du bassin vocontien (S-E de la France). *Geobios*, 28: 357-365.

Reboulet S., Mattioli E., Pictet B., Baudin F., Olivero D. & Proux O. (2003). Ammonoid and nannoplankton abundance in Valanginian (early Cretaceous) limestone–marl successions from the southeast France Basin: carbonate dilution or productivity? *Palaeogeography, Palaeoclimatology, Palaeoecology*, 201: 113-139.

Reboulet S., Giraud F. & Proux O. (2005). Ammonoid abundance variations related to changes in trophic conditions across the Oceanic Anoxic Event 1d (Latest Albian, SE France). *Palaios*, 20: 121-141.

Reboulet S., Szives O., Aguirre-Urreta B., Barragán R., Company M., Frau C., Kakabadze M.V., Klein J., Moreno-Bedmar J.A., Lukeneder A., Pictet A., Ploch I., Raisossadat S.N., Vašíček Z., Baraboshkin E.J. & Mitta V.V. (2017). Report on the 6th International meeting of the IUGS Lower Cretaceous Ammonite Working Group, the Kilian Group (Vienna, Austria, 20th August 2017). *Cretaceous Reserch*, 91: 100-110.

Reinhardt P. (1964). Einige Kalkflagellaten-Gattungen (Coccolithophoriden, Coccolithineen) aus dem Mesozoikum Deutschlands. *Monatsberichte der Deutschen Akademie der Wissenschaften zu Berlin*, 6: 749-759.

Reinhardt P. (1965). Neue Familien für fossile Kalkflagellaten (Coccolithophoriden, Coccolithineen). *Monatsberichte der Deutschen Akademie der Wissenschaften zu Berlin*, 7: 30-40.

Reinhardt P. (1966). Zur Taxonomie und Biostratigraphie des fossilen Nannoplanktons aus dem Malm, der Kreide und dem Alttertiär Mitteleuropas. *Freiberger Forschungshefte*, 196: 5-109.

Rieber H. (1977). Eine ammonitenfauna aus der oberen Maiolica der Breggia-schlucht (Tessin/Schweiz). *Eclogae Geologicae Helvetiae*, 70: 777-787.

Rood A.P., Hay W.W. & Barnard T. (1971). Electron Microscope Studies of Oxford Clay Coccoliths. *Eclogae Geologicae Helvetiae*, 64: 245-272.

Roth P.H. (1994). Distribution of coccoliths in oceanic sediments. *In* Winter A. & Siesser W.G. (eds), Coccolithophore. Cambridge University Press: 199-218.

Roth P.H. & Krumbach K.R. (1986). Middle Cretaceous calcareous nannofossil biogeography and presevation in the Atlantic and Indian oceans: implications for paleoceanography. *Marine Micropaleontology*, 10: 235-266.

Roveri M. & Taviani M. (2003). Calcarenite and sapropel deposition in the Mediterranean Pliocene: shallow-and deep-water record of astronomically driven climatic events. *Terra Nova*, 15: 279-286.

Royo Y Gomez J. (1945). Fosiles del Barremiense colombiano. *Compilaciones de los studios geologicos oficiales de Colombia*, 6: 455-495.

Santantonio M. (1993). Facies associations and evolution of pelagic carbonate platform/basin systems: Examples from the Italian Jurassic. *Sedimentology*, 40: 1039-1067.

Santantonio M. & Carminati E. (2011). Jurassic rifting evolution of the Apennines and Southern Alps (Italy): Parallels and differences. *Geological Society of America Bulletin*, 123: 468-484.

Sayn G. (1920). Les Phylloceras gargasiens du S.E. de la France (espèces nouvelles ou peuconnues). *Mémoire pour servir à l'explication de la carte géologique détaillée de la France*: 191-203.

Siesser W.G., Bralower T.J. & De Carlo E.H. (1992). Mid-Tertiary Braarudosphaera-rich sediments on the Exmouth Plateau. *In* von Rad U., Haq B.U. et al. (eds), Proceedings of the Ocean Drilling Program, Scientific Results, Texas A & M University, Ocean Drilling Program, College Station, 122: 653-663.

Sissing W. (1977). Biostratigraphy of the Cretaceous calcareous nannoplankton. *Geologie en Mijnbouw*, 56: 37-65.

Sissingh W. (2007). Biostratigraphy of Cretaceous calcareous nannoplankton. *Netherlands Journal of Geosciences*, 56: 37-65.

Spath L.F. (1923). Appendix: On ammonites from New Zealand. *In* Trechmann C.T. (ed.), The Jurassic rocks of New Zealand. *Quarterly Journal of the Geological Society of London*, 79: 286-308.

Spath L.F. (1924). On the ammonites of the Speeton Clay and the subdivisions of the Neocomian. *Geological Magazine*, 61: 73 89.

Spath L.F. (1925). Ammonites and aptychi. The collection of fossils and rocks from Somaliland. *Monographs Geological Department of the Hunterian Museum*, 1: 111-164.

Spath L.F. (1927). Revision of the Jurassic Cephalopod Fauna of Kachh (Cutch). Part 1. Memoirs of the Geological Survey of India. *Palaeontologia Indica*, 9: 1-71.

Sprovieri M., Coccioni R., Lirer F., Pelosi N. & Lozar F. (2006). Orbital tuning of a lower Cretaceous composite record (Maiolica Formation, central Italy). *Paleoceanography*, 21: 1-19.

Stahlecker R. (1935). Neocom auf der Kapverden-Insel Maio. *Neues Jahrbuch für Mineralogie, Geologie und Paläontologie*, 1934: 265-301.

Stradner H. (1963). New contributions to Mesozoic stratigraphy by means of nannofossils. *Proceedings of the Sixth World Petroleum Congress*, 1: 167-183.

Street C. & Bown P.R. (2000). Palaeobiogeography of early Cretaceous (Berriasien–Barremien) calcareous nannoplankton. *Marine Micropaleontology*, 39: 265-291.

Suess E. (1865). Uber Ammoniten. Sitzungsberichte der Kaiserlichen Akademie der Wissenschaften in Wien. *Mathematisch-Naturwissenschaftliche*, 52: 71-89.

Szives O., Moreno-Bedmar J., Aguirre-Urreta B., Company M., Frau C., López-Horgue M., Pictet A., Ploch I., Salazar C., Barragán R., Latil J.L., Lehmann J., Robert E. & Reboulet S. (2023). Report on the 7th International Meeting of the IUGS Lower Cretaceous Ammonite Working Group, the Kilian Group (Warsaw, Poland, 21st August 2022): State of the art on the current Standard Ammonite Zonation of the Western Tethyan Mediterranean Province. *Cretaceous Research*, 153: 105716.

Talbi R., Amri A., Boujemaa A., Gabtni H., Spiller R. & Levey R. (2021). First evidence of the early Cretaceous oceanic anoxic events (MBE and OAE1a) in the southern Tethyan margin (NE-Tunisia): biostratigraphy and shale resource system. *Journal of Petroleum Exploration and Production*, 11: 1559-1575.

Thieuloy J.P. (1966). Leptocères berriasiens du massif de la Grande-Chartreuse. *Géologie Alpine*, 42: 281-295.

Thierstein H.R. (1971). Tentative Lower Cretaceous Calcareous Nannoplankton Zonation. *Eclogae Geologicae Helvetiae*, 64: 459-488.

Thierstein H.R. (1973). Lower Cretaceous calcareous nannoplankton biostratigraphy. *Abhandlungen der Geologischen Bundesanstalt*, 29: 3-52.

Thierstein H.R. (1981). Late Cretaceous nannoplankton and the change at the Cretaceous-Tertiary boundary. *Society of Economic Paleontologists and Mineralogists, Special Publication*, 32: 355-394.

Thierstein H.R. & Roth P.H. (1991). Stable isotopic and carbonate cyclicity in Lower Cretaceous deep-sea sediments: dominance of diagenetic effects. *Marine Geology*, 97: 1-34.

Tiraboschi D. & Erba E. (2010). Calcareous nannofossil biostratigraphy (Upper Bajocian–Lower Bathonian) of the Ravin du Bès section (Bas Auran, Subalpine Basin, SE France): evolutionary trends of *Watznaueria barnesiae* and new findings of "*Rucinolithus*" morphotypes. *Geobios*, 43: 59-76.

Trejo M. (1969). Conusphaera mexicana, un nuevo coccolitoforido del Jurassico Superior de Mexico. *Revista del Instituto Mexicano del Petroleo*, 1: 5-15.

Tremolada F. & Erba E. (2002). Morphometric analyses of Aptian *Assipetra infracretacea* and *Rucinolithus terebrodentarius* nannoliths: implications for taxonomy, biostratigraphy and paleoceanography. *Marine Micropaleontology*, 44: 77-92.

Tremolada F., Erba E. & Bralower T.J. (2006). Late Barremian to early Aptian calcareous nannofossil paleoceanography and paleoecology from the Ocean Drilling Program Hole 641C (Galicia Margin). *Cretaceous Research*, 27: 887-897.

Tremolada F., Erba E., De Bernardi B. & Cecca F. (2009). Calcareous nannofossil fluctuations during the late Hauterivian in the Cismon core (Venetian Alps, northeastern Italy) and in selected sections of the Umbria-Marche Basin (central Italy): paleoceanographic implications of the Faraoni Level. *Cretaceous Research*, 30: 505-514.

Turco E., Schettino A., Nicosia U., Santantonio M., Di Stefano P., Iannace A., Cannata D., Conti M.A., Deiana G., D'Orazi Porchetti S., Felici F., Liotta D., Mariotti M., Milia A., Petti F.M., Pierantoni P.P., Sacchi E., Sbrescia V., Tommasetti K., Valentini M., Zamparelli V. & Zarcone G. (2007). Mesozoic Paleogeography of the Central Mediterranean Region. Geoitalia 2007, VI Forum Italiano di Scienze della Terra. *Epitome*, 2: 108.

Uhlig V. (1882). Die Wernsdorfer Schichten und ihre Aquivalente. *Sitzungsberichre der Kaiserlichen Akademie der Weissenscheften in Wien, Mathematisch-Naturwissenshaftliche*, 86: 86-117.

Uhlig V. (1883). Die Cephalopodenfauna der Wernsdorfer Schichten. *Denkschriften der Kaiserlichen Akademie der Weissenscheften in Wien, Mathematisch-Naturwissenshaftliche*, 46: 127-290.

Uhlig V. (1905). Einige Bemarkungen uber die Ammonitengattung Hoplites Neumayer. *Sitzungsberichre der Kaiserlichen Akademie der Weissenscheften in Wien, Mathematisch-Naturwissenshaftliche*, 144: 591-636.

Uhlig V. (1910). The fauna of the Spiti Shales. Memoirs of the Geological Survey of India. *Palaeontologia Indica*, 15: 133-306.

Vašíček Z. & Hoedemaeker P.J. (2003). A new Karsteniceras from the Barremian (Lower Cretaceous) of Colombia. *Scripta Geologica*, 125: 141-143.

Vašíček Z. & Klajmon P. (1998). Contribution to the knowledge of some small Early Barremian ammonites from the Silesian Unit (Outer Carpathians, Czech Republic). *Věstník Českého geologického ústavu*, 73: 331-342.

Vašíček Z. & Wiedmann J. (1994). The Leptoceratoidinae: small heteromorph ammonites from the Barremian. *Palaeontology*, 37: 203-239.

Vermeulen J. (1996). Kotetishvilia, nouveau genre barrémien de la sous-famille des. *Géologie Alpine*, 72: 117-125.

Verri A. (1883). Appunti sul bacino del Cascio e del Topino. *Bollettino della Società Geologica Italiana*, 2: 108-125.

Westermann G.E.G. (1990). New developments in ecology of Jurassic-Cretaceous ammonoids. *In* Pallini G., Cecca F., Cresta S. & Santantonio M. (eds), Fossili, Evoluzione, Ambiente. Atti Convegno (Pergola), 1987: 459-478.

Westermann G.E.G. (1996). Ammonoid Life and Habitat. *In* Landman N.H., Tanabe K. & Davis R.A. (eds), Ammonoid paleobiology. *Topics in Geobiology*, 13: 607-707.

Wieczorek J. (1988). Maiolica-a unique facies of the Western Tethys. *Annales Societatis Geologorum Poloniae*, 58: 255-276.

Wiedmann J. (1978). On the significance of ammonite nuclei from sieve residues. *Annales des Mines et de la Géologie*, 28: 135-161.

Williams J.R. & Bralower T.J. (1995). Nannofossil assemblages, fine fraction stable isotopes, and the paleoceanography of the Valanginian-Barremian (Early Cretaceous) North Sea Basin. *Paleoceanography*, 10: 815-839.

Wippich M.G. & Lehmann J. (2004). Allocrioceras from the Cenomanian (mid-Cretaceous) of the Lebanon and its bearing on the palaeobiological interpretation of heteromorphic ammonites. *Palaeontology*, 47: 1093-1107.

Wouters S., Schnyder J., Satolli S., Martinez M., Boulvain F., Goovaerts T., Meyvis B., & Devleeschouwer X. (2018). Progressive increase in organic-matter burial and preservation from the "Weissert" event to the Faraoni event in Umbria-Marche (central Italy). *In* 6th International Geologica Belgica Meeting 2018 (KU Leuven, 2018). https://hdl.handle.net/2268/229963

Wright C., Callamon J.H. & Howarth M.K. (1996). Cretaceous Ammonoidea. *In* Kaesler R.L. (ed.), Treatise on invertebrate paleontology. Part L. Mollusca 4 Revised: 1-392.

Wulff L., Mutterlose J. & Bornemann A. (2020). Size variations and abundance patterns of calcareous nannofossils in mid Barremian black shales of the Boreal Realm (Lower Saxony Basin). *Marine Micropaleontology*, 156: 101853.

Yilmaz I.O., Altiner D., Tekin U.K. & Ocakoglu F. (2012). The first record of the "Mid-Barremian" Oceanic Anoxic Event and the Late Hauterivian platform drowning of the Bilecik platform, Sakarya Zone, western Turkey. *Cretaceous Research*, 38: 16-39.

Young J.R., Bown P.R. & Lees J.A. (2022). *Nannotax3 website*. International Nannoplankton Association. Accessed 9 September 2024. www.mikrotax.org/Nannotax3

Zittel K.A. (1870). Studio geologico nell'Appennino Centrale. *Bollettino del Regio Comitato Geologico d'Italia*, 1: 17-28.

Zittel K.A. (1895). Grundzuge der Palaeontologie. Oldenbourg. Munich & Liepzig, 8: 1-971.

Manuscript submitted 8 January 2025
Revised manuscript accepted 1 October 2025

Editor Silvia Danise